



1 Terpenes and their oxidation products in the French Landes forest: 2 insight from Vocus PTR-TOF measurements

3 Haiyan Li¹, Matthieu Riva², Pekka Rantala¹, Liine Heikkinen¹, Kaspar Daellenbach¹, Jordan E.
4 Krechmer³, Pierre-Marie Flaud^{4,5}, Douglas Worsnop³, Markku Kulmala¹, Eric Villenave^{4,5}, Emilie
5 Perraudin^{4,5}, Mikael Ehn¹, Federico Bianchi¹

6 ¹ Institute for Atmospheric and Earth System Research / Physics, Faculty of Science, University of Helsinki, Finland

7 ² Univ. Lyon, Université Claude Bernard Lyon 1, CNRS, IRCELYON, F-69626, Villeurbanne, France

8 ³ Aerodyne Research Inc., Billerica, Massachusetts 01821, USA

9 ⁴ Univ. Bordeaux, EPOC, UMR 5805, F-33405 Talence Cedex, France

10 ⁵ CNRS, EPOC, UMR 5805, F-33405 Talence Cedex, France

11 Correspondence: Haiyan Li (haiyan.li@helsinki.fi) and Matthieu Riva (matthieu.riva@ircelyon.univ-lyon1.fr)

12 **Abstract.** The capabilities of the recently developed Vocus proton-transfer-reaction time-of-flight mass spectrometer (PTR-
13 TOF) are reported for the first time based on ambient measurements. With the deployment of the Vocus PTR-TOF, we present
14 an overview of the observed gas-phase (oxygenated) molecules in the French Landes forest during summertime 2018 and gain
15 insights into the atmospheric oxidation of terpenes, which are emitted in large quantities in the atmosphere and play important
16 roles in secondary organic aerosol production. Due to the greatly improved detection efficiency compared to traditional PTR
17 instruments, the Vocus PTR-TOF identifies a large amount of gas-phase signals with elemental composition categories
18 including CH, CHO, CHN, CHS, CHON, CHOS, and others. Multiple hydrocarbons are detected, with carbon numbers up to
19 20. Particularly, we report the first direct observations of low-volatility diterpenes in the ambient air. The diurnal cycle of
20 diterpenes is similar to that of monoterpenes and sesquiterpenes, but contrary to that of isoprene. Various types of terpene
21 reaction products and intermediates are also characterized. Generally, the more oxidized products from terpene oxidations
22 show a broad peak in the day due to the strong photochemical effects, while the less oxygenated products peak in the early
23 morning and/or in the evening. To evaluate the importance of different formation pathways in terpene chemistry, the reaction
24 rates of terpenes with main oxidants (i.e., hydroxyl radical, OH; ozone, O₃; and nitrate radical, NO₃) are calculated. For the
25 less oxidized non-nitrate monoterpene oxidation products, their morning peaks likely have contributions from both O₃- and
26 OH-initiated monoterpene oxidation. Due to the decreased OH concentration at night, monoterpene ozonolysis becomes more
27 important in the evening. For the monoterpene-derived organic nitrates, oxidations by O₃, OH, and NO₃ radicals all contribute
28 to their formation, with their relative roles varying considerably over the course of the day. Through a detailed analysis of
29 terpene chemistry, this study demonstrates the capability of the Vocus PTR-TOF in the detection of a wide range of oxidized
30 reaction products in ambient and remote conditions, which highlights its importance in investigating atmospheric oxidation
31 processes.

32 1. Introduction

33 Organic aerosol (OA) constitutes a large fraction of atmospheric particles, having significant impacts on climate change, air
34 quality, and human health (Maria et al., 2004; IPCC, 2013; Mauderly and Chow, 2008). On a global scale, secondary OA
35 (SOA) is the largest source of OA, formed through the oxidation of volatile organic compounds (VOCs) (Jimenez et al., 2009).
36 Biogenic VOCs (BVOCs) are released into the atmosphere in high amounts, with an annual global budget being 760 Tg C
37 (Sindelarova et al., 2014). On average, SOA production from biogenic precursors ranges from 2.5 to 44.5 Tg C annually, which
38 is much larger than that from anthropogenic sources (Tsigaridis and Kanakidou, 2003). Over the past few years, a considerable
39 amount of studies have been conducted to investigate the atmospheric chemistry of BVOCs (Calfapietra et al., 2013; Jokinen



40 et al., 2015; Ng et al., 2017). However, an incomplete understanding of BVOCs characteristics and their oxidation processes
41 in the atmosphere remains and yields large uncertainties in quantitative estimates of air quality and climate effects of
42 atmospheric aerosols (Carslaw et al., 2013; Zhu et al., 2019).

43 Terpenes make up the main fraction of BVOCs (Guenther et al., 1995), encompassing isoprene (C_5H_8), monoterpenes
44 ($C_{10}H_{16}$), sesquiterpenes ($C_{15}H_{24}$), diterpenes ($C_{20}H_{32}$) and even larger compounds. With one or more C=C double bonds in
45 their molecular structures, terpenes are highly reactive. After entering the atmosphere, terpenes can undergo oxidative
46 chemistry with the common atmospheric oxidants including hydroxyl radical (OH), ozone (O_3), and nitrate radical (NO_3).
47 These oxidation processes generate a large variety of organic species, with volatilities ranging from gas-phase volatile species
48 (VOC), to semi-volatile / low volatility organic compounds (SVOC and LVOC), to extremely low volatility organic
49 compounds (ELVOC), which irretrievably contribute to SOA formation (Donahue et al., 2012). Due to the chemical
50 complexity and low concentrations of BVOCs oxidation products, it remains extremely challenging to provide a
51 comprehensive understanding of terpene chemistry in the atmosphere.

52 With a high time response and sensitivity, proton-transfer-reaction mass spectrometry (PTR-MS) has been widely
53 used to study the emissions and chemical evolution of VOCs in the atmosphere (Yuan et al., 2017). However, due to
54 instrumental wall losses, previous PTR-MS instruments were not optimized to detect low volatility compounds. For example,
55 only a few ambient PTR-MS observations of sesquiterpenes are available (Kim et al., 2009; Jardine et al., 2011; Hellén et al.,
56 2018). Correspondingly, it is not surprising that ambient observations of diterpenes, which are generally considered to be non-
57 volatile compounds, have never been reported. In addition, the existing PTR-MS is often not sensitive enough to quantify
58 terpene oxidation products at atmospherically relevant concentrations (Yuan et al., 2017). To address these instrumental
59 limitations, two new versions of PTR were recently developed, the PTR3 (Breitenlechner et al., 2017) and the Vocus PTR-
60 TOF (Krechmer et al., 2018), both coupled with a time of flight (TOF) mass analyzer. With the drastically enhanced
61 sensitivities, these instruments are capable in detecting broader spectrum of VOCs, where the detection of low-volatility VOCs
62 is significantly improved compared to the traditional PTR-MS. Based on the laboratory evaluation by Riva et al. (2019a), the
63 Vocus PTR-TOF is able to measure both monoterpenes and lots of monoterpene oxidation products containing up to 6 oxygen
64 atoms.

65 Known for strong monoterpene emitters (Simon et al., 1994), the Landes forest in southwestern France is a suitable
66 place to investigate atmospheric terpene chemistry. A previous study at this site reported a high nocturnal monoterpene loading
67 and suggested that monoterpene oxidations play an important role in formation of new particles and the consequent growth of
68 atmospheric particles (Kammer et al., 2018). To better assess the roles of BVOCs in aerosol formation, the Characterization
69 of Emissions and Reactivity of Volatile Organic Compounds in the Landes Forest (CERVOLAND campaign) took place in
70 July 2018. The recently developed Vocus PTR-TOF was deployed in the CERVOLAND campaign to characterize terpenes
71 and their gas-phase oxidation products, which provides the first Vocus PTR-TOF measurement in a forested environment. In
72 this work, we present a comprehensive summary of the identified gas-phase molecules and gain insights into terpene chemistry
73 to demonstrate the Vocus PTR-TOF capabilities and the importance of its applications in atmospheric sciences.
74 Characterizations of isoprene, monoterpenes, sesquiterpenes, and particularly the rarely detected diterpenes, are reported. By
75 comparing the reaction rates of different formation pathways, we explore the formation mechanisms of terpene oxidation
76 products, including both non-nitrate and organic nitrate compounds.

77 2. Experimental methods

78 2.1 Measurement site

79 The Vocus PTR-TOF measurements were performed from 8 to 20 July, 2018 in the Landes forest ($44^{\circ}29'39.69''N$,
80 $0^{\circ}57'21.75''W$), as part of the CERVOLAND field campaign. The sampling site is situated at the European Integrated Carbon



81 Observation System (ICOS) station at Bilos in southwestern France along the Atlantic coast, ~40 km southwest from the
82 nearest urban area of the Bordeaux metropole. A detailed description of the site has been given by Moreaux et al. (2011).
83 Briefly, both population density and industrial emissions are low in this area. The forest is largely composed of maritime pines,
84 known as a strong monoterpene emitter (Simon et al., 1994), which provides a good place for BVOCs characterization.

85 2.2 Instrumentation

86 Compared to the traditional PTR instrument, the Vocus PTR-TOF used in this study is mainly differentiated in the following
87 aspects:

- 88 1. a new chemical ionization source with a low-pressure reagent-ion source and focusing ion-molecule reactor (FIMR),
- 89 2. no dependence of the sensitivity on ambient sample humidity due to the high water mixing ratio (10-20 % v/v) in the
90 FIMR,
- 91 3. employment of a TOF mass analyzer with a longer flight tube and faster sampling data acquisition card (mass
92 resolving power up to 15 000 m/dm),
- 93 4. an enhanced inlet and source design that minimizes contact between analyte molecules and inlet/source walls,
94 enabling detection of semi- and low-volatility compounds in a similar manner as chemical ionization mass
95 spectrometer (CIMS) instruments (Liu et al. 2019).

96
97 Details about the Vocus PTR-TOF are well described by Krechmer et al. (2018). Compared to the ionization in a traditional
98 PTR-MS at 2.0-4.0 mbar, a nitrate CIMS at ambient pressure, and an iodide CIMS at around 100 mbar, we operate the Vocus
99 ionization source at a low pressure of 1.0-1.5 mbar. During the campaign, the Vocus PTR-TOF measurements were performed
100 at around 2 m above ground level (a.g.l). Sample air was drawn in through 1-m long PTFE tubing (10 mm o.d., 8 mm i.d.)
101 with a flow rate of 4.5 L min⁻¹, which helped to reduce inlet wall losses and sampling delay. Of the total sample flow, only
102 150 sccm went into the Vocus, while the remainder was directed to the exhaust. The design of FIMR consists of a glass tube
103 with a resistive coating on the inside surface and four quadrupole rods mounted radially on the outside. With an RF field, ions
104 are collimated to the central axis, improving the detection efficiency of product ions. The mass resolving power of the 1.2 m
105 long TOF mass analyzer was 12 000-13 000 m/dm during the whole campaign. Data were recorded with a time resolution of
106 5 s. Background measurements using high purity nitrogen (UHP N₂) were automatically performed every hour.

107 The temperature, relative humidity (RH), wind speed, and ambient pressure were continuously monitored at 3.4 m
108 a.g.l. whereas the solar radiation was measured at 15.6 m a.g.l from a mast located at the site. The mixing ratios of nitrogen
109 oxides (NO_x) and ozone (O₃) were measured at 4 m a.g.l with UV absorption and chemiluminescence analyzers, respectively.
110 All data are reported in Coordinated Universal Time (UTC).

111 2.3 Data analysis and quantification of multiple compounds

112 Data analysis was performed using the software package “Tofware” (<https://www.tofwerk.com/software/tofware/>) that runs in
113 the Igor Pro environment (WaveMetrics, OR, USA). Tofware enables the time-dependent mass calibration, baseline
114 subtraction, and assignment of a molecular formula to the identified ions by high resolution analysis. Signals were averaged
115 over 30 min before mass calibration. Due to the high resolving power of the LTOF mass analyzer, isobaric ions were more
116 clearly separated. Examples of peak identification are given in Fig. S1.

117 The Vocus was calibrated twice a day during the campaign with a mixture (70 ppb each) of terpenes (*m/z* 137:
118 alpha/beta pinene + limonene; *m/z* 135: cymene) that was diluted using UHP N₂. Similar to traditional PTR instrument, the
119 sensitivities for different VOCs in the Vocus are linearly related to their rate constants of the proton-transfer reactions
120 (Cappellin et al., 2012; Krechmer et al., 2018). Using the calculated sensitivities of monoterpenes and cymene from calibration
121 data and their respective rate constants (*k*), an empirical relationship between the sensitivity and *k* was built from the



122 scatterplots using linear regression: Sensitivity = $509.75 \times k$. Once k is available, the sensitivity of a compound can be predicted.
123 It should be noted that both monoterpenes and cymene fragment inside the instrument. The predicted sensitivities with this
124 method may be underestimated for compounds which do not fragment or fragment less than monoterpenes and cymene inside
125 the PTR instruments. Rate constants for the proton-transfer reactions have only been measured for a subset of compounds. To
126 quantify terpenes and their oxidation products, we used the method proposed by Sekimoto et al. (2017) to calculate the rate
127 constants of different compounds with the polarizability and permanent dipole moment of the molecule. According to
128 Sekimoto et al. (2017), the polarizability and dipole moment of a molecule can be obtained based on the molecular mass,
129 elemental composition, and functionality of the compound. For a class of VOCs with the same number of electronegative
130 atoms, their polarizabilities can be well described using their molecular mass (Sekimoto et al., 2017). For VOCs containing a
131 specific functional group, it is found that their dipole moments are relatively constant based on results in the CRC Handbook
132 (Lide, 2005). Since no isomer information is provided by mass spectrometry alone, it is challenging to figure out the
133 functionality of different compounds. Therefore, the polarizability and dipole moment of the compounds observed in this study
134 were estimated only based on the molecular mass and elemental composition. In this work, based on the physical properties
135 of various compounds in CRC Handbook (Lide, 2005) and the results in Sekimoto et al. (2017), we built the functions between
136 polarizability (α) and molecular mass (M_R) for different groups of VOCs and calculated the average dipole moment (μ) for
137 each group. For example, the polarizabilities of hydrocarbons were approximated as $\alpha = 0.142 M_R - 0.3$ and the dipole moment
138 was approximated to be zero. For the non-nitrate oxygenated compounds with one oxygen, $\alpha = 0.133 M_R - 1.2$, and the dipole
139 moment was averaged to be 1.6.

140 It should be noted that uncertainties are introduced to the calculated sensitivities in the following factors. First,
141 oxidized compounds usually fragment more than terpene precursors in PTR instruments. For instance, alcohol-containing
142 compounds easily split off water and undergo the highest degree of fragmentation (Buhr et al., 2002). A study by Kari et al.
143 (2018) showed that around 95.5% of 1,8 - cineole fragmented with an reduced electric field (E/N) of 130 Td. Molecules
144 containing other functional groups fragment to varying, but lesser degrees; however, the theoretically calculated sensitivities
145 here should be regarded as upper limits for terpene oxidation products. Further, some low-volatility compounds may
146 experience wall losses to varying extents inside the inlet tubing and the instrument and therefore have worse transmissions.
147 The method in this work may overestimate the sensitivities of these low-volatility compounds. In addition to proton transfer
148 reactions, some VOCs can be ionized through ligand switching reactions with water cluster ($(H_2O)_nH_3O^+$) (Tani et al., 2004),
149 thus increasing their sensitivity. However, with the calibration standards used in this study, it is hard to estimate the effect of
150 ligand switching ionization. Lastly, uncertainties come from the estimation of polarizability and dipole moment of a molecule.
151 With the method used in this study, the sensitivity is calculated to be within 50% error when only the elemental composition
152 of a compound is known (Sekimoto et al., 2017).

153 3. Results and discussion

154 3.1 Meteorology and trace gases

155 Figure 1 displays the time variations of meteorological conditions and trace gases during the observation period. The weather
156 was mostly sunny, with solar radiation varying from 400 to 800 W/m² during daytime, indicating strong photochemical activity.
157 The ambient temperature and RH varied regularly every day. On average, the temperature was 22.8 ± 5.9 °C, ranging from
158 12.1 to 35.0 °C, which is favorable for BVOCs emissions in the forest. The average RH was 70.5 ± 19.0 % during the campaign.
159 Generally, the air masses were quite stable within the canopy. The wind speed never exceeded 1 m/s, indicating the major
160 influence of local sources on atmospheric processes in this study.

161 The O₃ levels fluctuated dramatically between day and night during the campaign. The average O₃ diurnal cycle
162 showed that O₃ concentration peaked up to ~50 ppb in the daytime. However, during most of the nights, O₃ concentration



163 dropped below 2 ppb. Considering the high nighttime concentration of terpenes observed by the previous study at this site in
164 the same season (Kammer et al., 2018), the low O₃ level at night suggests the full consumption of O₃ by terpenes. Such
165 reactions of terpenes with O₃ can produce low volatility organic compounds, thus contributing to SOA formation (Presto et al.,
166 2005; Jokinen et al., 2014).

167 The NO concentration was generally low during the campaign, below detection limit (i.e., <0.5 ppb) most of the time.
168 However, clear NO plumes was sometimes observed in the early morning, as shown in Fig. 1e. The NO concentration peak at
169 4 am is probably the combination of local emission sources and low boundary layer. With the increasing sunlight afterwards,
170 the NO concentration started to decrease. A similar diel pattern of NO₂ was observed by the previous study at this site (Kammer
171 et al., 2018). The lower NO₂ concentration during daytime is likely explained by dilution with increasing boundary layer height
172 and NO₂ photolysis.

173 3.2 Vocus PTR-TOF capabilities in the forest

174 While Krechmer et al. (2018) and Riva et al. (2019a) have described the novel setup and performance of the Vocus PTR-TOF
175 and its application during a lab study, the instrument capability has not been fully explored in an ambient environment. Based
176 on the CERVOLAND deployment, we provide here, the first overview of gas-phase molecules measured by the Vocus PTR-
177 TOF in the forest. For a better visualization of the complex data set from real atmosphere, mass defect plots (averaged over
178 the whole campaign) are shown in Fig. 2 with the difference between the accurate mass and the nominal mass of a compound
179 plotted against its accurate mass. With the addition of hydrogen atoms, the mass defect increases, while the addition of oxygen
180 atoms decreases the mass defect. Therefore, changes in the mass defect plot help to provide information on chemical
181 transformation such as oxidation.

182 The mass defect plot in Fig. 2a is colored according to the retrieved elemental composition, with the black circle
183 indicating unidentified molecules. The size of the markers is proportional to the logarithm of the peak area of the molecule.
184 During the campaign, the Vocus PTR-TOF detected large amounts of (O)VOCs, with elemental composition categories of CH,
185 CHO, CHN, CHS, CHON, CHOS, and others. For hydrocarbons, multiple series with different carbon numbers were measured,
186 with compounds containing 5 carbon atoms (“C₅”), 10 carbon atoms (“C₁₀”), 15 carbon atoms (“C₁₅”), and 20 carbon atoms
187 (“C₂₀”) highlighted in the figure. Compared to the traditional PTR instruments, the observation of larger hydrocarbon
188 molecules by the Vocus PTR-TOF is mainly caused by the much lower wall losses and increased detection efficiency.
189 Hydrocarbon signals were largely contributed by monoterpene (C₁₀H₁₆H⁺) and its major fragment (C₆H₈H⁺), indicating the
190 monoterpene-dominated environment in the Landes forest (Kammer et al., 2018). According to previous studies, monoterpene
191 emissions in the Landes forest are dominated by α-pinene and β-pinene (Simon et al., 1994; Kammer et al., 2018). The
192 identified compound with the elemental composition of C₄H₉⁺ ranked the third largest peak in hydrocarbons. One possible
193 explanation for C₄H₉⁺ peak could be the protonated butene, which is emitted by vegetations or from anthropogenic sources
194 (Goldstein et al., 1996; Zhu et al., 2017). The fragmentation of butanol also produces C₄H₉⁺ signal. Like many other alcohols,
195 butanol can easily lose an OH during ionization in PTR sources (Spanel and Smith, 1997). During the measurements at the
196 Station for Measuring Ecosystem-Atmosphere Relations (SMEAR II) site in Hyytiälä, Finland, Schallhart et al. (2018)
197 concluded that C₄H₉⁺ signal detected by PTR-TOF mainly came from butanol used by aerosol instruments, i.e., condensation
198 particle counters (CPCs). In this study, CPCs using butanol to measure the particle concentration were also deployed at the
199 site. While the exhaust air emitted from these collocated instruments was filtered using charcoal denuder, we cannot exclude
200 the contribution of butanol to the identified C₄H₉⁺ signal. The spiky peaks in the time series of C₄H₉⁺ compound also indicated
201 the influence of butanol (Fig. S2). Finally, the green leaf volatiles (GLV), a group of six-carbon aldehyde, alcohols and their
202 esters which can be directly released by the plants, have been found to fragment at *m/z* 57 inside the PTR instruments (Rinne
203 et al., 2005; Pang, 2015) and may also contribute to the observed C₄H₉⁺ signal.



204 In addition to the emitted precursors, the Vocus PTR-TOF detected various VOCs reaction products and
205 intermediates. Similar to the PTR3 measurements in the CLOUD chamber (Breitenlechner et al., 2017), many oxygenated
206 compounds from terpene reactions with varying degrees of oxidation were observed in this study. However, as a potential
207 limitation of the instrument, no dimers in the atmosphere were identified by the Vocus PTR-TOF, consistent with the results
208 from a previous laboratory deployment (Riva et al., 2019a). Several cyclic volatile methyl siloxanes (VMS) were measured,
209 which have been recently reported by traditional PTR-TOF instruments (Yuan et al., 2017). Cyclic VMS are silicon-containing
210 compounds widely used in cosmetics and personal care products (Buser et al., 2013; Yucuis et al., 2013). In this study, the
211 identified peaks of cyclic VMS were protonated D3 siloxane ($C_6H_{18}O_3Si_3$), D4 siloxane ($C_8H_{24}O_4Si_4$), D5 siloxane
212 ($C_{10}H_{30}O_5Si_5$), D6 siloxane ($C_{12}H_{36}O_6Si_6$), and their H_3O^+ cluster ions. The existence of these peaks in the mass spectra helps
213 to extend the range in mass or peak-width calibrations.

214 Figure 2b compares the daytime and nighttime variations of different molecules, with the marker sized by the signal
215 difference between day and night. The daytime periods cover from 4:30 am to 7:30 pm, and the nighttime periods are from
216 7:30 pm to 4:30 am of the next day (both are UTC time). The data points are colored in orange when the nighttime signal of
217 the compound is larger than its daytime signal, and in green when the daytime signal is higher. Patterns in the figure clearly
218 show the difference in the diurnal variations of gas molecules with different oxidation degrees. For example, most
219 hydrocarbons are characterized with higher concentrations at night, which is largely caused by the stable nocturnal boundary
220 layer. The more oxidized compounds with more oxygen numbers are generally more abundant during the day due to enhanced
221 photochemistry, whereas the concentrations of the less oxidized compounds are mostly higher at night. Details on the diurnal
222 profiles of different oxidation products and their formation mechanisms are provided in Sect. 3.4.

223 3.3 Terpene characteristics

224 The characterizations of isoprene, monoterpenes, sesquiterpenes, and the rarely reported diterpenes, are investigated in this
225 study (Fig. 3, Fig. 4). On the global scale, isoprene is the most emitted BVOC species. It has been well established that
226 photooxidation of isoprene in the atmosphere contributes to SOA formation through the multiphase reactions of isoprene-
227 derived oxidation products (Claeys et al., 2004; Henze and Seinfeld, 2006; Surratt et al., 2010). However, recent advances on
228 isoprene chemistry found that isoprene can impact both particle number and mass of monoterpene-derived SOA by scavenging
229 hydroxyl and peroxy radicals (Kiendler-Scharr et al., 2009; Kanawade et al., 2011; McFiggans et al., 2019). During the
230 CERVOLAND campaign, the average mixing ratio of isoprene was 0.6 ppb, consistent with the mean value of 0.4 ppb reported
231 for the LANDEX campaign during summer 2017 at the same site (Mermet et al., 2019). These values are much lower than that
232 in the southeastern United States (Xiong et al., 2015) and Amazon rainforest (Wei et al., 2018) but higher than observations
233 in the boreal forest at the SMEAR II station (Hellén et al., 2018). Isoprene emissions require sunlight (Monson et al., 1989).
234 Therefore, a pronounced diurnal pattern of isoprene was observed with maximum mixing ratios occurring during daytime and
235 minima at night.

236 As expected, monoterpenes showed the highest mixing ratios among all the terpenes, with an average value of 6.0
237 ppb. On July 9, a heavy monoterpene episode occurred at night, with the monoterpene mixing ratio reaching as high as 41.2
238 ppb. Comparatively, the average monoterpene level observed in this work is similar to the measurements performed in 2015
239 and 2017 at the same site (Kammer et al., 2018; Mermet et al., 2019) and more than ten times higher than that observed in the
240 boreal forest at SMEAR II in summer (Hakola et al., 2012; Hellén et al., 2018). The high concentration of monoterpenes
241 indicates the potential significance of monoterpene-related aerosol chemistry in the Landes forest. Opposite to the diurnal
242 variations of isoprene, monoterpene concentrations peaked at night, caused by the stable nocturnal boundary layer. During
243 daytime, the concentration of monoterpenes dropped to around 0.9 ppb, due to the increased atmospheric mixing after sunrise
244 and the rapid photochemical consumptions.



245 A study in Hyttiälä concluded that sesquiterpenes, due to their higher reactivity, could play a more important role in
246 O₃ chemistry than monoterpenes, even though the concentration of sesquiterpenes was much lower (Hellén et al., 2018).
247 However, the short lifetimes of sesquiterpenes also mean that their concentrations will be highly dependent on the sampling
248 location at a given site. Some studies also proposed that sesquiterpene oxidation products are linked to atmospheric new particle
249 formation (Bonn and Moortgat, 2003; Boy et al., 2007). Despite the potential importance of sesquiterpenes in aerosol chemistry,
250 the available data on ambient sesquiterpene quantification remains still quite limited. In this work, the mixing ratios of
251 sesquiterpenes were found to vary from 8.9 ppt to 408.9 ppt in the Landes forest, with an average of 64.5 ppt during the
252 observations. This sesquiterpene level is comparable to that reported by Mermet et al. (2019) in summer 2017 at the same site
253 and observations by Jardine et al. (2011) in Amazonia but higher than previous measurements at SMEAR II station (Hellén et
254 al., 2018). As shown in Fig. 4, sesquiterpenes displayed a similar diurnal pattern with monoterpenes, consistent with
255 observations in other areas (Jardine et al., 2011; Hellén et al., 2018).

256 While diterpenes are present in all plants in the form of phytol, they have been thought for a long time not to be
257 released by vegetation due to their low volatility (Keeling and Bohmann, 2006). In 2004, von Schwarzenberg et al. (2004)
258 reported for the first time the release of plant-derived diterpenes into the air. A recent study found that the emission rate of
259 diterpenes by Mediterranean vegetation was in the same order of magnitude as monoterpenes and sesquiterpenes (Yáñez-
260 Serrano et al., 2018). For the first time, this study reports the ambient concentration of diterpenes in a forest. According to the
261 Vocus PTR-TOF measurements, the average mixing ratio of diterpenes was around 2 ppt in the Landes forest. Considering the
262 low volatility of diterpenes and their potential wall losses inside the inlet tubing and the instrument, the diterpene concentration
263 might be higher. Similar to monoterpenes and sesquiterpenes, diterpenes presented peak concentrations at night and lower
264 levels during the day. Although the amounts of diterpenes in the atmosphere are hundreds to thousands times lower than those
265 of monoterpenes and sesquiterpenes, diterpenes potentially play a role in atmospheric chemistry due to their unsaturated
266 structure and high molecular weight (Matsunaga et al., 2012). Up to now, there is no report on the possible atmospheric
267 implications of diterpenes, which should deserve more attention in the future.

268 Considering the similar atmospheric behaviors of monoterpenes, sesquiterpenes, and diterpenes in this study, it is
269 questioned if the observed sesquiterpenes and diterpenes are real signals in the atmosphere or generated by monoterpenes in
270 the instrument. Figure 5 illustrates the scatter plots among monoterpenes, sesquiterpenes, and diterpenes, colored by time of
271 the day. At night, both sesquiterpenes and diterpenes correlated well with monoterpenes. However, their correlation with
272 monoterpenes got weaker during daytime as the data points became more scattered. This suggests that the observations of
273 sesquiterpenes and diterpenes are real emissions in the atmosphere. Comparatively, sesquiterpenes and diterpenes showed a
274 strong correlation with each other through the whole day ($r^2 = 0.85$).

275 3.4 Insights into terpene chemistry

276 3.4.1 Comparison with chamber results

277 Due to the diverse precursors and changing environmental conditions in the ambient air, it is challenging to retrieve all the
278 atmospheric chemical processes occurring within the Landes forest. To start with, we compare the ambient data with those
279 from α -pinene ozonolysis in the presence of NO_x conducted in the COALA chamber at the University of Helsinki. A detailed
280 description of the laboratory experiment is provided elsewhere (Riva et al., 2019a, 2019b). According to literature,
281 monoterpenes undergo some degree of fragmentation within the PTR instrument, producing dominant ions of C₆H₉⁺, C₅H₇⁺,
282 C₇H₁₁⁺, et al (Tani et al., 2003, 2013; Kari et al., 2018). As illustrated in Fig. 6, C₆H₉⁺ is the largest fragment produced by
283 monoterpenes within the Vocus PTR-TOF. However, a clear difference of monoterpene fragmentation pattern is observed in
284 the mass spectra of ambient observations and chamber experiments. While the signal of C₆H₉⁺ is lower than that of C₁₀H₁₇⁺
285 during the field deployment, C₆H₉⁺ peak is higher than C₁₀H₁₇⁺ peak in the chamber study. Based on the monoterpene
286 calibration data, the C₆H₉⁺ signal is around 40% and 138% of the protonated monoterpene signal in ambient deployment and



287 chamber experiment, respectively. The larger presence of the $C_6H_9^+$ peak in the chamber study can be likely explained by the
288 much higher concentrations of oxygenated terpenoids during the chamber experiments. Indeed, previous studies have shown
289 that oxygenated terpenoids, including linalool and pinonaldehyde, fragment inside the PTR instrument and produce a dominant
290 ion at m/z 81 (Maleknia et al., 2007; Tani, 2013). Different settings of the instrument in the two studies can also contribute to
291 the difference, i.e., the Vocus pressure, the drift voltage, and different mass transmission functions of the instrument (Tani et
292 al., 2003, 2013; Kari et al., 2018). In addition, the fragmentation patterns vary among individual monoterpene species due to
293 their different physicochemical properties (Tani et al., 2013; Kari et al., 2018). Considering that α -pinene is the only
294 monoterpene species injected in the chamber experiment, the combination of various monoterpenes in the atmosphere likely
295 introduces additional differences in the fragmentation pattern.

296 Gas-phase ozonolysis of alkenes generates OH radicals in high yields (Rickard et al., 1999). Without an OH scavenger,
297 both O_3 - and OH-initiated oxidations happened during α -pinene ozonolysis in the chamber. Using the Vocus PTR-TOF,
298 various oxidation products were identified in the chamber study, with the dominant species being $C_7H_{10,12}O_{3-6}$, $C_8H_{14}O_{3-6}$,
299 $C_9H_{14}O_{1-5}$, and $C_{10}H_{14,16}O_{2-6}$. In comparison, more oxygenated compounds which were directly emitted or from monoterpene
300 reactions were observed in ambient air due to complex environmental conditions, with the oxygen number ranging from 1 to
301 7. Therefore, the Vocus PTR-TOF measurements provide the opportunity to characterize both the emitted precursors and the
302 resulting oxidation products. During the chamber experiments, NO_2 was injected and photolyzed using 400nm LED lights to
303 generate NO. In the presence of NO_x , organic nitrates were formed from the reactions between NO and monoterpene-derived
304 peroxy radicals (RO_2). The major organic nitrates observed were $C_9H_{13,15}NO_{6-8}$ and $C_{10}H_{13,15}NO_{3-8}$. Compared to the chamber
305 study, more organic nitrates of C_8 , C_9 , and C_{10} from monoterpene reactions were identified in CERVOLAND data. It is worth
306 pointing out that the combination of different monoterpene species in the ambient environment may result in various types of
307 organic nitrates through different formation pathways.

308 3.4.2 Non-nitrate terpene oxidation products

309 Based on the ambient observations, the non-nitrate oxidation products from isoprene, monoterpenes, and sesquiterpenes, are
310 investigated in this study. Isoprene gas-phase products are mainly represented by C_4 and C_5 compounds (Wennberg et al.,
311 2018). In this work, we consider $C_4H_{6,8}O_n$ and $C_5H_{8,10,12}O_n$ ($n=1\sim 6$) as the dominant non-nitrate products from isoprene
312 oxidations. The diurnal variations of $C_5H_8O_n$ are displayed in Fig. 7 and the others in Fig. S3-5. Generally, all these oxidation
313 products displayed an evening peak at around 8 pm, which may come from the O_3 - or OH-initiated isoprene oxidations.
314 Globally, reactions with O_3 contribute a small fraction of approximately 10% to isoprene removal in the atmosphere (Wennberg
315 et al., 2018). When isoprene reacts with O_3 , one carbon is always split off from the molecule (Criegee, 1975). Considering the
316 peak concentration of isoprene at 8 pm and the relatively high O_3 concentration at the moment (Figs. 1 and 4), isoprene
317 ozonolysis is likely contributing to the formation of C_4 oxidation products. Because OH radicals can be efficiently produced
318 from alkene ozonolysis (Pfeiffer et al., 2001), the OH-initiated oxidation of isoprene can also be an important formation
319 pathway of these oxidation products in the evening. For example, as a predominant product from the reactions of isoprene with
320 OH, $C_5H_{10}O_3$ (corresponding to isoprene hydroxy hydroperoxide and/or isoprene epoxydiols) presented a clear single peak in
321 the evening. To determine the relative importance of O_3 - and OH-initiated oxidations in isoprene chemistry at night, the
322 reaction rate (R) of isoprene with O_3 and OH radical were compared by Eq. (1) and Eq. (2):

$$323 R_{ISO+OH} = k_{ISO+OH}[ISO][OH] \quad (1)$$

$$324 R_{ISO+O_3} = k_{ISO+O_3}[ISO][O_3] \quad (2)$$

325 where k is the reaction rate coefficient of isoprene with OH or O_3 , and [ISO], [OH] or [O_3] is the concentration of isoprene,
326 OH radical or O_3 .

327 Taking the evening peak of isoprene oxidation products at 8 pm as an example, we compared the roles of O_3 and OH radicals
328 in their formation. Laboratory studies have shown that the reaction rate coefficient of isoprene with OH radical is generally



329 10^7 times larger than that of isoprene with O_3 (Dreyfus et al., 2002; Kari et al., 2004). According to literature, the nighttime
330 concentration of tropospheric OH radical varies in the range of $1 \times 10^4 - 1 \times 10^5$ molecules cm^{-3} (0.0004 – 0.004 ppt) in the
331 field (Shirinzadeh et al., 1987; Khan et al., 2008; Petäjä et al., 2009; Stone et al., 2012). Therefore, with an O_3 concentration
332 of ~20 ppb at 8 pm, if the OH concentration was around 1×10^4 molecule cm^{-3} (0.0004 ppt) at the moment, the reaction rate
333 of isoprene with OH radical was around 0.2 times as high as that of isoprene with O_3 . If the OH concentration reached up to 1
334 $\times 10^5$ molecule cm^{-3} (0.004 ppt) at 8 pm, the reaction rate of isoprene with OH radical was 2 times higher than that of isoprene
335 with O_3 . For the more oxidized compounds from isoprene oxidations, their concentrations had a broad daytime presence from
336 10 am to 8 pm due to strong photooxidation processes. Similar diurnal variations of $C_4H_6,8O_{5,6}$ and $C_5H_{8,10,12}O_{5,6}$ measured by
337 nitrate CIMS have been observed in an isoprene-dominated environment at Centreville, Alabama (Massoli et al., 2018).

338 The diurnal patterns of $C_8H_{12,14}O_n$, $C_9H_{14}O_n$, and $C_{10}H_{14,16,18}O_n$ ($n=1\sim6$) were illustrated to characterize monoterpene
339 oxidations in the Landes forest (Fig. 8; Fig. S6-10). For the less oxidized compounds with oxygen numbers from 1 to 4, most
340 of them were observed with clear morning and evening peaks, which can be produced from O_3 - and OH-initiated monoterpene
341 oxidations. For the morning peak at around 7 am, the relative roles of O_3 - and OH-initiated monoterpene oxidation were
342 evaluated using the similar method as in Eq. (1) and Eq. (2). The reaction rate coefficient of monoterpene + OH is
343 approximately 10^6 times higher than that of monoterpene + O_3 (Atkinson et al., 1990; Khamaganov and Hites, 2001; Gill and
344 Hites, 2002; Hakola et al., 2012). In the morning, typical tropospheric OH concentrations have been observed to be around 1
345 $\times 10^5 - 1 \times 10^6$ molecule cm^{-3} (0.004 – 0.04 ppt) (Shirinzadeh et al., 1987; Ren et al., 2003; Khan et al., 2008; Petäjä et al.,
346 2009; Stone et al., 2012). For an OH concentration of 1×10^5 molecule cm^{-3} (0.004 ppt), with the average O_3 concentration of
347 15 ppb at 7 am, the reaction rate of monoterpene + OH was about 0.25 times as high as that of monoterpene + O_3 . If the OH
348 concentration was up to 1×10^6 molecule cm^{-3} (0.04 ppt) at 7 am, the reaction rate of monoterpene with OH radical was 2.5
349 times higher than that of monoterpene with O_3 according to the calculations. In other words, both oxidants are likely to be of
350 importance at this time. For the evening peak of the less oxidized monoterpene oxidation products at 8 pm, the relative
351 importance of O_3 and OH radical in monoterpene chemistry changed due to the lower OH concentration. With the average O_3
352 concentration of ~20 ppb at 8 pm, a similar analysis as above resulted in O_3 reactions being 5-50 times more important than
353 OH radical reactions with monoterpenes, indicating that the evening peaks are mainly from ozonolysis. Compared to other
354 compounds, the evening peak of $C_9H_{14}O$, $C_{10}H_{16}O$, $C_{10}H_{18}O$, and $C_{10}H_{18}O_2$ extended over midnight. $C_9H_{14}O$ has been found
355 to be one of the main products formed in the ozonolysis reactions of monoterpenes (Atkinson and Arey, 2003). O_3 -initiated
356 oxidation with extremely high monoterpene levels might be responsible for the high concentration of $C_9H_{14}O$ at night.
357 Camphor ($C_{10}H_{16}O$), linalool ($C_{10}H_{18}O$), and linalool oxide ($C_{10}H_{18}O_2$) can be emitted by leaves and flowers (Corchnoy et al.,
358 1992; Lavy et al., 2002). Therefore, direct emissions from vegetation in the Landes forest may contribute to the high mixing
359 ratios of these compounds during night. With strong photochemical oxidations during the day, the diurnal cycles of the more
360 oxidized compounds were characterized with a broad daytime distribution peaking between 2:00 pm and 4:00 pm UTC.

361 To date the oxidation processes of sesquiterpenes have been rarely investigated despite its potential significance in
362 new particle formation and SOA formation (Bonn and Moortgat, 2003; Winterhalter et al., 2009). In this study, various
363 sesquiterpene oxidation products were observed, mainly including $C_{14}H_{22}O_n$, $C_{15}H_{22}O_n$, and $C_{15}H_{24}O_n$ ($n=1\sim6$), providing the
364 possibility to explore the oxidations of sesquiterpenes in the atmosphere. As shown in Fig. 9 and Fig. S11-12, with the increase
365 of oxygen numbers, sesquiterpene oxidation products displayed similar variations in their diurnal profiles with monoterpene
366 oxidation products. The less oxidized products with 1 to 3 oxygen peaked both in the morning and in the evening, and the
367 more oxidized compounds had a broad presence throughout the day. These results indicate the similar oxidation processes of
368 sesquiterpenes with monoterpenes in the Landes forest.



369 3.4.3 Terpene-derived organic nitrates

370 Organic nitrates have been shown to represent a large fraction of submicron aerosol nitrate at both urban and rural sites in
371 Europe (Kiendler-Scharr et al., 2016). During daytime, the reaction of peroxy radicals with NO can lead to the formation of
372 organic nitrates. At night, NO₃ radicals from the oxidation of NO₂ by O₃, can also react with unsaturated compounds mostly
373 coming from BVOCs to generate organic nitrates (Ayres et al., 2015). In this study, the less oxidized organic nitrates from
374 monoterpene oxidations presented a distinct morning peak at 7 am (Fig. 11; Fig. S15-16), which can come from O₃- and OH-
375 initiated monoterpene oxidations in the presence of NO_x. In addition, both isoprene- and monoterpene-derived organic nitrates
376 showed evening peaks at around 8 pm (Fig. 10, Fig. S13-14). Using monoterpenes as an example, the relative roles of O₃, OH
377 radical, and NO₃ radical in the nighttime formation of monoterpene-derived organic nitrates were evaluated by calculating the
378 corresponding reaction rate (R):

$$379 R_{\text{MT}+\text{O}_3} = k_{\text{MT}+\text{O}_3}[\text{MT}][\text{O}_3] \quad (3)$$

$$380 R_{\text{MT}+\text{OH}} = k_{\text{MT}+\text{OH}}[\text{MT}][\text{OH}] \quad (4)$$

$$381 R_{\text{MT}+\text{NO}_3} = k_{\text{MT}+\text{NO}_3}[\text{MT}][\text{NO}_3] \quad (5)$$

382 where k is the reaction rate coefficient of monoterpenes with O₃, OH radical or NO₃ radical, and [MT], [O₃], [OH] or [NO₃] is
383 the concentration of monoterpenes, O₃, OH radical or NO₃ radical.

384 Taking the peak concentration of monoterpene-derived organic nitrates at 8 pm as an example, the concentration of NO₃ radical
385 was calculated by assuming a steady state between its production from O₃ and NO₂ and its removal by oxidation reactions and
386 losses. The details have been described by Allan et al. (2000) and Peräkylä et al. (2014). With the high O₃ scavenging by
387 monoterpenes in the evening, the estimated concentration of NO₃ radical was 0.017 ppt. Using $k_{\text{MT}+\text{O}_3} = 6.9 \times 10^{-17} \text{ cm}^3$
388 $\text{molecule}^{-1} \text{ s}^{-1}$ and $k_{\text{MT}+\text{NO}_3} = 7.5 \times 10^{-12} \text{ cm}^3 \text{ molecule}^{-1} \text{ s}^{-1}$ taken from Peräkylä et al. (2014), the reaction rate of monoterpenes
389 with O₃ was ~10 times higher than that of monoterpenes with NO₃ radicals. However, while ozonolysis was likely to dominate
390 the overall oxidation of monoterpenes, the organic nitrate formation from O₃-initiated oxidation may still be much lower than
391 those from NO₃-initiated oxidations, depending on what fraction of RO₂ radicals were reacting with NO_x. The relative
392 importance of O₃ and OH radical in monoterpene chemistry at this time was the same as discussed in Sect. 3.4.2.

393 4. Conclusions

394 This work presented the deployment of the new state-of-the-art Vocus PTR-TOF in the French Landes forest during the
395 CERVOLAND campaign. The Vocus PTR-TOF capabilities are evaluated for the first time in the actual ambient environment
396 by the identification of the observed gas-phase molecules. With the improved detection efficiency and measurement precision
397 compared to the traditional PTR instruments, multiple hydrocarbons with carbon numbers varying from 3 to 20 were observed
398 as well as various VOCs oxidation products. Hydrocarbon signals were dominated by monoterpenes and their major fragment
399 ions (e.g., C₆H₈H⁺) within the instrument, consistent with high monoterpene emissions in the Landes forest. In general, most
400 hydrocarbon molecules and the less oxidized compounds were characterized with high signals at night, whereas the more
401 oxidized compounds exhibited elevated intensity during the day.

402 To demonstrate the importance of Vocus PTR-TOF application in atmospheric science study, the characteristics of
403 terpenes and their oxidation products were investigated. In addition to the observation of isoprene, monoterpenes, and
404 sesquiterpenes, this study presented the ambient characteristics of the rarely recorded diterpenes, which are traditionally
405 considered as non-volatile species in the atmosphere. On average, the concentration of diterpenes was 1.7 ppt in the Landes
406 forest, which was hundred to thousand times lower than that of monoterpenes (6.0 ppb) and sesquiterpenes (64.5 ppt). However,
407 considering their low vapor pressure and high reactivity, diterpenes may potentially play an important part in atmospheric
408 chemistry. The diurnal variations of diterpenes showed the maximum peak at night and low levels during the day, similar to
409 those of monoterpenes and sesquiterpenes.



410 With strong photochemical oxidations of terpenes during the day, the more oxidized terpene reaction products were
411 observed with a broad daytime peak, whereas the less oxidized terpene reaction products showed peak concentrations in the
412 early morning or/and in the evening. By calculating the reaction rates of terpenes with the main oxidants, OH radical, O₃, and
413 NO₃ radical, the contributions of different formation pathways to terpene oxidations were evaluated. The morning peaks of
414 non-nitrate terpene reaction products were contributed by both O₃- and OH-induced terpene oxidations. For the evening peaks
415 of non-nitrate terpene oxidation products, terpene ozonolysis played an increasing role due to the lower OH concentration at
416 night. For the formation of terpene-derived organic nitrates, the relative importance of O₃-, OH-, and NO₃- driven oxidation
417 pathways were more difficult to evaluate. Overall, we have shown that the Vocus PTR-TOF is able to detect a very broad
418 coverage of compounds, from VOCs precursors to various oxidation products. Therefore, the application of the Vocus PTR-
419 TOF in atmospheric sciences will be fundamental in understanding the chemical evolution of VOCs in the atmosphere and
420 their roles in air quality and climate issues.

421 **Author contributions**

422 ME and MR conceived the study. MR, LH, PF, EV, and EP conducted the field measurements. HL carried out the data analysis.
423 MR, PR, KD, JK, DW, MK, ME, and FB participated the data analysis. HL wrote the paper with inputs from all coauthors.

424 **Competing interests**

425 The authors declare that they have no conflict of interest.

426 **Acknowledgements**

427 This work was supported by the European Research Council under grants 742206 ATM-GP and 638703 COALA, and the
428 Academy of Finland (project numbers 317380 and 320094). The authors would like to thank the PRIMEQUAL programme
429 for financial support (ADEME, convention #1662C0024). This study has also been carried out with financial support from the
430 French National Research Agency (ANR) in the frame of the Investments for the future Programme, within the Cluster of
431 Excellence COTE (ANR-10-LABX-45) of the University of Bordeaux. Special thanks to Dr Elena Ormeño-Lafuente (IMBE)
432 for the loan of the BVOC calibration gas cylinders and Dr Christophe Chipeaux and Dr Denis Loustau (ISPA-INRA) for their
433 precious help in providing meteorological data and access to ICOS station facility.

434 **References**

- 435 Atkinson, R., Hasegawa, D., and Aschmann, S. M.: Rate constants for the gas-phase reactions of O₃ with a series of
436 monoterpenes and related compounds at 296 ± 2 K, *International Journal of Chemical Kinetics*, 22, 871-887,
437 10.1002/kin.550220807, 1990.
- 438 Atkinson, R., and Arey, J.: Atmospheric Degradation of Volatile Organic Compounds, *Chem Rev*, 103, 4605-4638,
439 10.1021/cr0206420, 2003.
- 440 Ayres, B. R., Allen, H. M., Draper, D. C., Brown, S. S., Wild, R. J., Jimenez, J. L., Day, D. A., Campuzano-Jost, P., Hu, W.,
441 de Gouw, J., Koss, A., Cohen, R. C., Duffey, K. C., Romer, P., Baumann, K., Edgerton, E., Takahama, S., Thornton, J. A.,
442 Lee, B. H., Lopez-Hilfiker, F. D., Mohr, C., Wennberg, P. O., Nguyen, T. B., Teng, A., Goldstein, A. H., Olson, K., and Fry,
443 J. L.: Organic nitrate aerosol formation via NO₃ + biogenic volatile organic compounds in the southeastern
444 United States, *Atmos. Chem. Phys.*, 15, 13377-13392, 10.5194/acp-15-13377-2015, 2015.
- 445 Baltensperger, U., Kalberer, M., Dommen, J., Paulsen, D., Alfarra, M. R., Coe, H., Fisseha, R., Gascho, A., Gysel, M., Nyeki,
446 S., Sax, M., Steinbacher, M., Prevot, A. S. H., Sjögren, S., Weingartner, E., and Zenobi, R.: Secondary organic aerosols from
447 anthropogenic and biogenic precursors, *Faraday Discussions*, 130, 265-278, 10.1039/B417367H, 2005.



- 448 Bernhammer, A. K., Fischer, L., Mentler, B., Heinritzi, M., Simon, M., and Hansel, A.: Production of highly oxygenated
449 organic molecules (HOMs) from trace contaminants during isoprene oxidation, *Atmos. Meas. Tech.*, 11, 4763-4773,
450 10.5194/amt-11-4763-2018, 2018.
- 451 Bertram, T. H., Kimmel, J. R., Crisp, T. A., Ryder, O. S., Yatavelli, R. L. N., Thornton, J. A., Cubison, M. J., Gonin, M., and
452 Worsnop, D. R.: A field-deployable, chemical ionization time-of-flight mass spectrometer, *Atmos. Meas. Tech.*, 4, 1471-1479,
453 10.5194/amt-4-1471-2011, 2011.
- 454 Bianchi, F., Kurtén, T., Riva, M., Mohr, C., Rissanen, M. P., Roldin, P., Berndt, T., Crouse, J. D., Wennberg, P. O., Mentel,
455 T. F., Wildt, J., Junninen, H., Jokinen, T., Kulmala, M., Worsnop, D. R., Thornton, J. A., Donahue, N., Kjaergaard, H. G., and
456 Ehn, M.: Highly Oxygenated Organic Molecules (HOM) from Gas-Phase Autoxidation Involving Peroxy Radicals: A Key
457 Contributor to Atmospheric Aerosol, *Chem Rev*, 10.1021/acs.chemrev.8b00395, 2019.
- 458 Bonn, B., and Moortgat, G. K.: Sesquiterpene ozonolysis: Origin of atmospheric new particle formation from biogenic
459 hydrocarbons, 30, doi:10.1029/2003GL017000, 2003.
- 460 Boy, M., Bonn, B., Maso, M. D., Hakola, H., Hirsikko, A., Kulmala, M., Kurtén, T., Laakso, L., Mäkelä, J., Riipinen, I.,
461 Rannik, Ü., Sihto, S.-L., and Ruuskanen, T. M.: Biogenic Sesquiterpenes and Atmospheric New Particle Formation: A Boreal
462 Forest Site Investigation, *Nucleation and Atmospheric Aerosols*, Dordrecht, 2007, 344-349,
- 463 Boyd, C. M., Sanchez, J., Xu, L., Eugene, A. J., Nah, T., Tuet, W. Y., Guzman, M. I., and Ng, N. L.: Secondary organic aerosol
464 formation from the β -pinene + NO₃ system: effect of humidity and peroxy radical fate, *Atmos. Chem. Phys.*, 15, 7497-7522,
465 10.5194/acp-15-7497-2015, 2015.
- 466 Breitenlechner, M., Fischer, L., Hainer, M., Heinritzi, M., Curtius, J., and Hansel, A.: PTR3: An Instrument for Studying the
467 Lifecycle of Reactive Organic Carbon in the Atmosphere, *Analytical Chemistry*, 89, 5824-5831,
468 10.1021/acs.analchem.6b05110, 2017.
- 469 Buhr, K., van Ruth, S., and Delahunty, C.: Analysis of volatile flavour compounds by Proton Transfer Reaction-Mass
470 Spectrometry: fragmentation patterns and discrimination between isobaric and isomeric compounds, *International Journal of*
471 *Mass Spectrometry*, 221, 1-7, [https://doi.org/10.1016/S1387-3806\(02\)00896-5](https://doi.org/10.1016/S1387-3806(02)00896-5), 2002.
- 472 Buser, A. M., Kierkegaard, A., Bogdal, C., MacLeod, M., Scheringer, M., and Hungerbühler, K.: Concentrations in Ambient
473 Air and Emissions of Cyclic Volatile Methylsiloxanes in Zurich, Switzerland, *Environmental Science & Technology*, 47,
474 7045-7051, 10.1021/es3046586, 2013.
- 475 Calfapietra, C., Fares, S., Manes, F., Morani, A., Sgrigna, G., and Loreto, F.: Role of Biogenic Volatile Organic Compounds
476 (BVOC) emitted by urban trees on ozone concentration in cities: A review, *Environ Pollut*, 183, 71-80,
477 <https://doi.org/10.1016/j.envpol.2013.03.012>, 2013.
- 478 Cappellin, L., Karl, T., Probst, M., Ismailova, O., Winkler, P. M., Soukoulis, C., Aprea, E., Märk, T. D., Gasperi, F., and
479 Biasioli, F.: On Quantitative Determination of Volatile Organic Compound Concentrations Using Proton Transfer Reaction
480 Time-of-Flight Mass Spectrometry, *Environmental Science & Technology*, 46, 2283-2290, 10.1021/es203985t, 2012.
- 481 Carlton, A. G., Wiedinmyer, C., and Kroll, J. H.: A review of Secondary Organic Aerosol (SOA) formation from isoprene,
482 *Atmos. Chem. Phys.*, 9, 4987-5005, 10.5194/acp-9-4987-2009, 2009.
- 483 Carslaw, K. S., Lee, L. A., Reddington, C. L., Pringle, K. J., Rap, A., Forster, P. M., Mann, G. W., Spracklen, D. V.,
484 Woodhouse, M. T., Regayre, L. A., and Pierce, J. R.: Large contribution of natural aerosols to uncertainty in indirect forcing,
485 *Nature*, 503, 67, 10.1038/nature12674, 2013.
- 486 Claeys, M., Graham, B., Vas, G., Wang, W., Vermeylen, R., Pashynska, V., Cafmeyer, J., Guyon, P., Andreae, M. O., Artaxo,
487 P., and Maenhaut, W.: Formation of Secondary Organic Aerosols Through Photooxidation of Isoprene, 303, 1173-1176,
488 10.1126/science.1092805 %J *Science*, 2004.
- 489 Corchnoy, S. B., Arey, J., and Atkinson, R.: Hydrocarbon emissions from twelve urban shade trees of the Los Angeles,
490 California, Air Basin, *Atmospheric Environment. Part B. Urban Atmosphere*, 26, 339-348, [https://doi.org/10.1016/0957-1272\(92\)90009-H](https://doi.org/10.1016/0957-1272(92)90009-H), 1992.
- 492 Criegee, R.: Mechanism of Ozonolysis, *Angewandte Chemie International Edition in English*, 14, 745-752,
493 10.1002/anie.197507451, 1975.
- 494 Crouse, J. D., McKinney, K. A., Kwan, A. J., and Wennberg, P. O.: Measurement of Gas-Phase Hydroperoxides by Chemical
495 Ionization Mass Spectrometry, *Analytical Chemistry*, 78, 6726-6732, 10.1021/ac0604235, 2006.



- 496 Donahue, N. M., Kroll, J. H., Pandis, S. N., and Robinson, A. L.: A two-dimensional volatility basis set – Part 2: Diagnostics
497 of organic-aerosol evolution, *Atmos. Chem. Phys.*, 12, 615–634, 10.5194/acp-12-615-2012, 2012.
- 498 Dreyfus, G. B., Schade, G. W., and Goldstein, A. H.: Observational constraints on the contribution of isoprene oxidation to
499 ozone production on the western slope of the Sierra Nevada, California, *Journal of Geophysical Research: Atmospheres*, 107,
500 ACH 1-1-ACH 1-17, 10.1029/2001JD001490, 2002.
- 501 Ehn, M., Kleist, E., Junninen, H., Petäjä, T., Lönn, G., Schobesberger, S., Dal Maso, M., Trimborn, A., Kulmala, M., Worsnop,
502 D. R., Wahner, A., Wildt, J., and Mentel, T. F.: Gas phase formation of extremely oxidized pinene reaction products in chamber
503 and ambient air, *Atmos. Chem. Phys.*, 12, 5113–5127, 10.5194/acp-12-5113-2012, 2012.
- 504 Ehn, M., Thornton, J. A., Kleist, E., Sipila, M., Junninen, H., Pullinen, I., Springer, M., Rubach, F., Tillmann, R., Lee, B.,
505 Lopez-Hilfiker, F., Andres, S., Acir, I. H., Rissanen, M., Jokinen, T., Schobesberger, S., Kangasluoma, J., Kontkanen, J.,
506 Nieminen, T., Kurten, T., Nielsen, L. B., Jorgensen, S., Kjaergaard, H. G., Canagaratna, M., Dal Maso, M., Berndt, T., Petaja,
507 T., Wahner, A., Kerminen, V. M., Kulmala, M., Worsnop, D. R., Wildt, J., and Mentel, T. F.: A large source of low-volatility
508 secondary organic aerosol, *Nature*, 506, 476–+, 2014.
- 509 Gill, K. J., and Hites, R. A.: Rate Constants for the Gas-Phase Reactions of the Hydroxyl Radical with Isoprene, α - and β -
510 Pinene, and Limonene as a Function of Temperature, *The Journal of Physical Chemistry A*, 106, 2538–2544,
511 10.1021/jp013532q, 2002.
- 512 Goldstein, A. H., Fan, S. M., Goulden, M. L., Munger, J. W., and Wofsy, S. C.: Emissions of ethene, propene, and 1-butene
513 by a midlatitude forest, 101, 9149–9157, doi:10.1029/96JD00334, 1996.
- 514 Guenther, A., Hewitt, C. N., Erickson, D., Fall, R., Geron, C., Graedel, T., Harley, P., Klinger, L., Lerdau, M., McKay, W. A.,
515 Pierce, T., Scholes, B., Steinbrecher, R., Tallamraju, R., Taylor, J., and Zimmerman, P.: A global model of natural volatile
516 organic compound emissions, *Journal of Geophysical Research: Atmospheres*, 100, 8873–8892, 10.1029/94JD02950, 1995.
- 517 Hakola, H., Tarvainen, V., Bäck, J., Ranta, H., Bonn, B., Rinne, J., and Kulmala, M.: Seasonal variation of mono- and
518 sesquiterpene emission rates of Scots pine, *Biogeosciences*, 3, 93–101, 10.5194/bg-3-93-2006, 2006.
- 519 Hakola, H., Hellén, H., Hemmilä, M., Rinne, J., and Kulmala, M.: In situ measurements of volatile organic compounds in a
520 boreal forest, *Atmos. Chem. Phys.*, 12, 11665–11678, 10.5194/acp-12-11665-2012, 2012.
- 521 Hallquist, M., Wängberg, I., Ljungström, E., Barnes, I., and Becker, K.-H.: Aerosol and Product Yields from NO₃ Radical-
522 Initiated Oxidation of Selected Monoterpenes, *Environmental Science & Technology*, 33, 553–559, 10.1021/es980292s, 1999.
- 523 Hellén, H., Praplan, A. P., Tykkä, T., Ylivinkka, I., Vakkari, V., Bäck, J., Petäjä, T., Kulmala, M., and Hakola, H.: Long-term
524 measurements of volatile organic compounds highlight the importance of sesquiterpenes for the atmospheric chemistry of a
525 boreal forest, *Atmos. Chem. Phys.*, 18, 13839–13863, 10.5194/acp-18-13839-2018, 2018.
- 526 Henze, D. K., and Seinfeld, J. H.: Global secondary organic aerosol from isoprene oxidation, 33, doi:10.1029/2006GL025976,
527 2006.
- 528 Hyttinen, N., Kupiainen-Määttä, O., Rissanen, M. P., Muuronen, M., Ehn, M., and Kurtén, T.: Modeling the Charging of
529 Highly Oxidized Cyclohexene Ozonolysis Products Using Nitrate-Based Chemical Ionization, *The Journal of Physical
530 Chemistry A*, 119, 6339–6345, 10.1021/acs.jpca.5b01818, 2015.
- 531 Intergovernmental Panel on Climate Change (IPCC), *Climate Change 2013: The Physical Science Basis. Contribution of
532 Working Group I to the Fifth Assessment Report of the Intergovernmental Panel on Climate Change*, 1535 pp., Cambridge
533 Univ. Press, Cambridge, U. K., and New York, 2013.
- 534 Isaacman-VanWertz, G., Massoli, P., O'Brien, R., Lim, C., Franklin, J. P., Moss, J. A., Hunter, J. F., Nowak, J. B., Canagaratna,
535 M. R., Misztal, P. K., Arata, C., Roscioli, J. R., Herndon, S. T., Onasch, T. B., Lambe, A. T., Jayne, J. T., Su, L. P., Knopf, D.
536 A., Goldstein, A. H., Worsnop, D. R., and Kroll, J. H.: Chemical evolution of atmospheric organic carbon over multiple
537 generations of oxidation, *Nat Chem*, 10, 462–468, 2018.
- 538 Jardine, K., Yañez Serrano, A., Arneeth, A., Abrell, L., Jardine, A., van Haren, J., Artaxo, P., Rizzo, L. V., Ishida, F. Y., Karl,
539 T., Kesselmeier, J., Saleska, S., and Huxman, T.: Within-canopy sesquiterpene ozonolysis in Amazonia, 116,
540 doi:10.1029/2011JD016243, 2011.
- 541 Jimenez, J. L., Canagaratna, M. R., Donahue, N. M., Prevot, A. S. H., Zhang, Q., Kroll, J. H., DeCarlo, P. F., Allan, J. D., Coe,
542 H., Ng, N. L., Aiken, A. C., Docherty, K. S., Ulbrich, I. M., Grieshop, A. P., Robinson, A. L., Duplissy, J., Smith, J. D., Wilson,
543 K. R., Lanz, V. A., Hueglin, C., Sun, Y. L., Tian, J., Laaksonen, A., Raatikainen, T., Rautiainen, J., Vaattovaara, P., Ehn, M.,
544 Kulmala, M., Tomlinson, J. M., Collins, D. R., Cubison, M. J., Dunlea, J., Huffman, J. A., Onasch, T. B., Alfarra, M. R.,



- 545 Williams, P. I., Bower, K., Kondo, Y., Schneider, J., Drewnick, F., Borrmann, S., Weimer, S., Demerjian, K., Salcedo, D.,
546 Cottrell, L., Griffin, R., Takami, A., Miyoshi, T., Hatakeyama, S., Shimono, A., Sun, J. Y., Zhang, Y. M., Dzepina, K., Kimmel,
547 J. R., Sueper, D., Jayne, J. T., Herndon, S. C., Trimborn, A. M., Williams, L. R., Wood, E. C., Middlebrook, A. M., Kolb, C.
548 E., Baltensperger, U., and Worsnop, D. R.: Evolution of Organic Aerosols in the Atmosphere, 326, 1525-1529,
549 10.1126/science.1180353 %J Science, 2009.
- 550 Jokinen, T., Sipilä, M., Richters, S., Kerminen, V.-M., Paasonen, P., Stratmann, F., Worsnop, D., Kulmala, M., Ehn, M.,
551 Herrmann, H., and Berndt, T.: Rapid Autoxidation Forms Highly Oxidized RO₂ Radicals in the Atmosphere, 53, 14596-14600,
552 doi:10.1002/anie.201408566, 2014.
- 553 Jokinen, T., Berndt, T., Makkonen, R., Kerminen, V.-M., Junninen, H., Paasonen, P., Stratmann, F., Herrmann, H., Guenther,
554 A. B., Worsnop, D. R., Kulmala, M., Ehn, M., and Sipilä, M.: Production of extremely low volatile organic compounds from
555 biogenic emissions: Measured yields and atmospheric implications, 112, 7123-7128, 10.1073/pnas.1423977112 %J
556 Proceedings of the National Academy of Sciences, 2015.
- 557 Kammer, J., Perraudin, E., Flaud, P. M., Lamaud, E., Bonnefond, J. M., and Villenave, E.: Observation of nighttime new
558 particle formation over the French Landes forest, *Sci Total Environ*, 621, 1084-1092,
559 <https://doi.org/10.1016/j.scitotenv.2017.10.118>, 2018.
- 560 Kanawade, V. P., Jobson, B. T., Guenther, A. B., Erupe, M. E., Pressley, S. N., Tripathi, S. N., and Lee, S. H.: Isoprene
561 suppression of new particle formation in a mixed deciduous forest, *Atmos. Chem. Phys.*, 11, 6013-6027, 10.5194/acp-11-
562 6013-2011, 2011.
- 563 Karl, M., Brauers, T., Dorn, H. P., Holland, F., Komenda, M., Poppe, D., Rohrer, F., Rupp, L., Schaub, A., and Wahner, A.:
564 Kinetic Study of the OH-isoprene and O₃-isoprene reaction in the atmosphere simulation chamber, SAPHIR, *Geophys Res
565 Lett*, 31, 10.1029/2003GL019189, 2004.
- 566 Kari, E., Miettinen, P., Yli-Pirilä, P., Virtanen, A., and Faiola, C. L.: PTR-ToF-MS product ion distributions and humidity-
567 dependence of biogenic volatile organic compounds, *International Journal of Mass Spectrometry*, 430, 87-97,
568 <https://doi.org/10.1016/j.ijms.2018.05.003>, 2018.
- 569 Keeling, C. I., and Bohmann, J.: Diterpene resin acids in conifers, *Phytochemistry*, 67, 2415-2423,
570 <https://doi.org/10.1016/j.phytochem.2006.08.019>, 2006.
- 571 Kesselmeier, J., and Staudt, M.: Biogenic Volatile Organic Compounds (VOC): An Overview on Emission, Physiology and
572 Ecology, *J Atmos Chem*, 33, 23-88, 10.1023/A:1006127516791, 1999.
- 573 Khamaganov, V. G., and Hites, R. A.: Rate Constants for the Gas-Phase Reactions of Ozone with Isoprene, α - and β -Pinene,
574 and Limonene as a Function of Temperature, *The Journal of Physical Chemistry A*, 105, 815-822, 10.1021/jp002730z, 2001.
- 575 Khan, M. A. H., Ashfold, M. J., Nickless, G., Martin, D., Watson, L. A., Hamer, P. D., Wayne, R. P., Canosa-Mas, C. E., and
576 Shallcross, D. E.: Night-time NO₃ and OH radical concentrations in the United Kingdom inferred from hydrocarbon
577 measurements, *Atmospheric Science Letters*, 9, 140-146, 10.1002/asl.175, 2008.
- 578 Kiendler-Scharr, A., Wildt, J., Maso, M. D., Hohaus, T., Kleist, E., Mentel, T. F., Tillmann, R., Uerlings, R., Schurr, U., and
579 Wahner, A.: New particle formation in forests inhibited by isoprene emissions, *Nature*, 461, 381, 10.1038/nature08292
580 <https://www.nature.com/articles/nature08292#supplementary-information>, 2009.
- 581 Kiendler-Scharr, A., Mensah, A. A., Friese, E., Topping, D., Nemitz, E., Prevot, A. S. H., Äijälä, M., Allan, J., Canonaco, F.,
582 Canagaratna, M., Carbone, S., Crippa, M., Dall'Osto, M., Day, D. A., De Carlo, P., Di Marco, C. F., Elbern, H., Eriksson, A.,
583 Freney, E., Hao, L., Herrmann, H., Hildebrandt, L., Hillamo, R., Jimenez, J. L., Laaksonen, A., McFiggans, G., Mohr, C.,
584 O'Dowd, C., Otjes, R., Ovadnevaite, J., Pandis, S. N., Poulain, L., Schlag, P., Sellegri, K., Swietlicki, E., Tiitta, P., Vermeulen,
585 A., Wahner, A., Worsnop, D., and Wu, H. C.: Ubiquity of organic nitrates from nighttime chemistry in the European submicron
586 aerosol, *Geophys Res Lett*, 43, 7735-7744, 10.1002/2016GL069239, 2016.
- 587 Kim, S., Karl, T., Helmig, D., Daly, R., Rasmussen, R., and Guenther, A.: Measurement of atmospheric sesquiterpenes by
588 proton transfer reaction-mass spectrometry (PTR-MS), *Atmos. Meas. Tech.*, 2, 99-112, 10.5194/amt-2-99-2009, 2009.
- 589 Kirkby, J., Duplissy, J., Sengupta, K., Frege, C., Gordon, H., Williamson, C., Heinritzi, M., Simon, M., Yan, C., Almeida, J.,
590 Tröstl, J., Nieminen, T., Ortega, I. K., Wagner, R., Adamov, A., Amorim, A., Bernhammer, A.-K., Bianchi, F., Breitenlechner,
591 M., Brilke, S., Chen, X., Craven, J., Dias, A., Ehrhart, S., Flagan, R. C., Franchin, A., Fuchs, C., Guida, R., Hakala, J., Hoyle,
592 C. R., Jokinen, T., Junninen, H., Kangasluoma, J., Kim, J., Krapf, M., Kürten, A., Laaksonen, A., Lehtipalo, K., Makhmutov,
593 V., Mathot, S., Molteni, U., Onnela, A., Peräkylä, O., Piel, F., Petäjä, T., Praplan, A. P., Pringle, K., Rap, A., Richards, N. A.
594 D., Riipinen, I., Rissanen, M. P., Rondo, L., Sarnela, N., Schobesberger, S., Scott, C. E., Seinfeld, J. H., Sipilä, M., Steiner,
595 G., Stozhkov, Y., Stratmann, F., Tomé, A., Virtanen, A., Vogel, A. L., Wagner, A. C., Wagner, P. E., Weingartner, E., Wimmer,



- 596 D., Winkler, P. M., Ye, P., Zhang, X., Hansel, A., Dommen, J., Donahue, N. M., Worsnop, D. R., Baltensperger, U., Kulmala,
597 M., Carslaw, K. S., and Curtius, J.: Ion-induced nucleation of pure biogenic particles, *Nature*, 533, 521, 10.1038/nature17953,
598 2016.
- 599 Krechmer, J., Lopez-Hilfiker, F., Koss, A., Hutterli, M., Stoermer, C., Deming, B., Kimmel, J., Warneke, C., Holzinger, R.,
600 Jayne, J., Worsnop, D., Fuhrer, K., Gonin, M., and de Gouw, J.: Evaluation of a New Reagent-Ion Source and Focusing Ion-
601 Molecule Reactor for Use in Proton-Transfer-Reaction Mass Spectrometry, *Analytical Chemistry*, 90, 12011-12018,
602 10.1021/acs.analchem.8b02641, 2018.
- 603 Lavy, M., Zuker, A., Lewinsohn, E., Larkov, O., Ravid, U., Vainstein, A., and Weiss, D.: Linalool and linalool oxide
604 production in transgenic carnation flowers expressing the *Clarkia breweri* linalool synthase gene, *Molecular Breeding*, 9, 103-
605 111, 10.1023/A:1026755414773, 2002.
- 606 Lee, B. H., Lopez-Hilfiker, F. D., Mohr, C., Kurten, T., Worsnop, D. R., and Thornton, J. A.: An Iodide-Adduct High-
607 Resolution Time-of-Flight Chemical-Ionization Mass Spectrometer: Application to Atmospheric Inorganic and Organic
608 Compounds, *Environmental Science & Technology*, 48, 6309-6317, 2014.
- 609 Lide, D. R. *CRC Handbook of Chemistry and Physics*; Internet Version 2005, <<http://www.hbcpnetbase.com>>, CRC Press,
610 Boca Raton, FL, 2005.
- 611 Liu, X., Deming, B., Pagonis, D., Day, D. A., Palm, B. B., Talukdar, R., Roberts, J. M., Veres, P. R., Krechmer, J. E., Thornton,
612 J. A., de Gouw, J. A., Ziemann, P. J., and Jimenez, J. L.: Effects of Gas-Wall Interactions on Measurements of Semivolatile
613 Compounds and Small Polar Molecules, *Atmos. Meas. Tech. Discuss.*, <https://doi.org/10.5194/amt-2019-52>, in review, 2019.
- 614 Maleknia, S. D., Bell, T. L., and Adams, M. A.: PTR-MS analysis of reference and plant-emitted volatile organic compounds,
615 *International Journal of Mass Spectrometry*, 262, 203-210, <https://doi.org/10.1016/j.ijms.2006.11.010>, 2007.
- 616 Maria, S. F., Russell, L. M., Gilles, M. K., and Myneni, S. C. B.: Organic Aerosol Growth Mechanisms and Their Climate-
617 Forcing Implications, 306, 1921-1924, 10.1126/science.1103491 %J Science, 2004.
- 618 Massoli, P., Stark, H., Canagaratna, M. R., Krechmer, J. E., Xu, L., Ng, N. L., Mauldin, R. L., Yan, C., Kimmel, J., Misztal,
619 P. K., Jimenez, J. L., Jayne, J. T., and Worsnop, D. R.: Ambient Measurements of Highly Oxidized Gas-Phase Molecules
620 during the Southern Oxidant and Aerosol Study (SOAS) 2013, *ACS Earth and Space Chemistry*, 2, 653-672,
621 10.1021/acsearthspacechem.8b00028, 2018.
- 622 Matsunaga, S. N., Chatani, S., Nakatsuka, S., Kusumoto, D., Kubota, K., Utsumi, Y., Enoki, T., Tani, A., and Hiura, T.:
623 Determination and potential importance of diterpene (kaur-16-ene) emitted from dominant coniferous trees in Japan,
624 *Chemosphere*, 87, 886-893, <https://doi.org/10.1016/j.chemosphere.2012.01.040>, 2012.
- 625 Mauderly, J. L., and Chow, J. C.: Health Effects of Organic Aerosols, *Inhalation Toxicology*, 20, 257-288,
626 10.1080/08958370701866008, 2008.
- 627 McFiggans, G., Mentel, T. F., Wildt, J., Pullinen, I., Kang, S., Kleist, E., Schmitt, S., Springer, M., Tillmann, R., Wu, C., Zhao,
628 D., Hallquist, M., Faxon, C., Le Breton, M., Hallquist, Å. M., Simpson, D., Bergström, R., Jenkin, M. E., Ehn, M., Thornton,
629 J. A., Alfarra, M. R., Bannan, T. J., Percival, C. J., Priestley, M., Topping, D., and Kiendler-Scharr, A.: Secondary organic
630 aerosol reduced by mixture of atmospheric vapours, *Nature*, 565, 587-593, 10.1038/s41586-018-0871-y, 2019.
- 631 Mermet, K., Sauvage, S., Dusanter, S., Salameh, T., Léonardis, T., Flaud, P.-M., Perraudin, É., Villenave, É., and Locoge, N.:
632 Optimization of a gas chromatographic unit for measuring BVOCs in ambient air, *Atmos. Meas. Tech. Discuss.*,
633 <https://doi.org/10.5194/amt-2019-224>, in review, 2019.
- 634 Monson, R. K., and Fall, R.: Isoprene Emission from Aspen Leaves, Influence of Environment and Relation to Photosynthesis
635 and Photorespiration, 90, 267-274, 10.1104/pp.90.1.267 %J Plant Physiology, 1989.
- 636 Moreaux, V., Lamaud, É., Bosc, A., Bonnefond, J.-M., Medlyn, B. E., and Loustau, D.: Paired comparison of water, energy
637 and carbon exchanges over two young maritime pine stands (*Pinus pinaster* Ait.): effects of thinning and weeding in the early
638 stage of tree growth, *Tree Physiology*, 31, 903-921, 10.1093/treephys/tptr048, 2011.
- 639 Ng, N. L., Brown, S. S., Archibald, A. T., Atlas, E., Cohen, R. C., Crowley, J. N., Day, D. A., Donahue, N. M., Fry, J. L.,
640 Fuchs, H., Griffin, R. J., Guzman, M. I., Herrmann, H., Hodzic, A., Iinuma, Y., Jimenez, J. L., Kiendler-Scharr, A., Lee, B.
641 H., Luecken, D. J., Mao, J., McLaren, R., Mutzel, A., Osthoff, H. D., Ouyang, B., Picquet-Varrault, B., Platt, U., Pye, H. O.
642 T., Rudich, Y., Schwantes, R. H., Shiraiwa, M., Stutz, J., Thornton, J. A., Tilgner, A., Williams, B. J., and Zaveri, R. A.:
643 Nitrate radicals and biogenic volatile organic compounds: oxidation, mechanisms, and organic aerosol, *Atmos. Chem. Phys.*,
644 17, 2103-2162, 10.5194/acp-17-2103-2017, 2017.



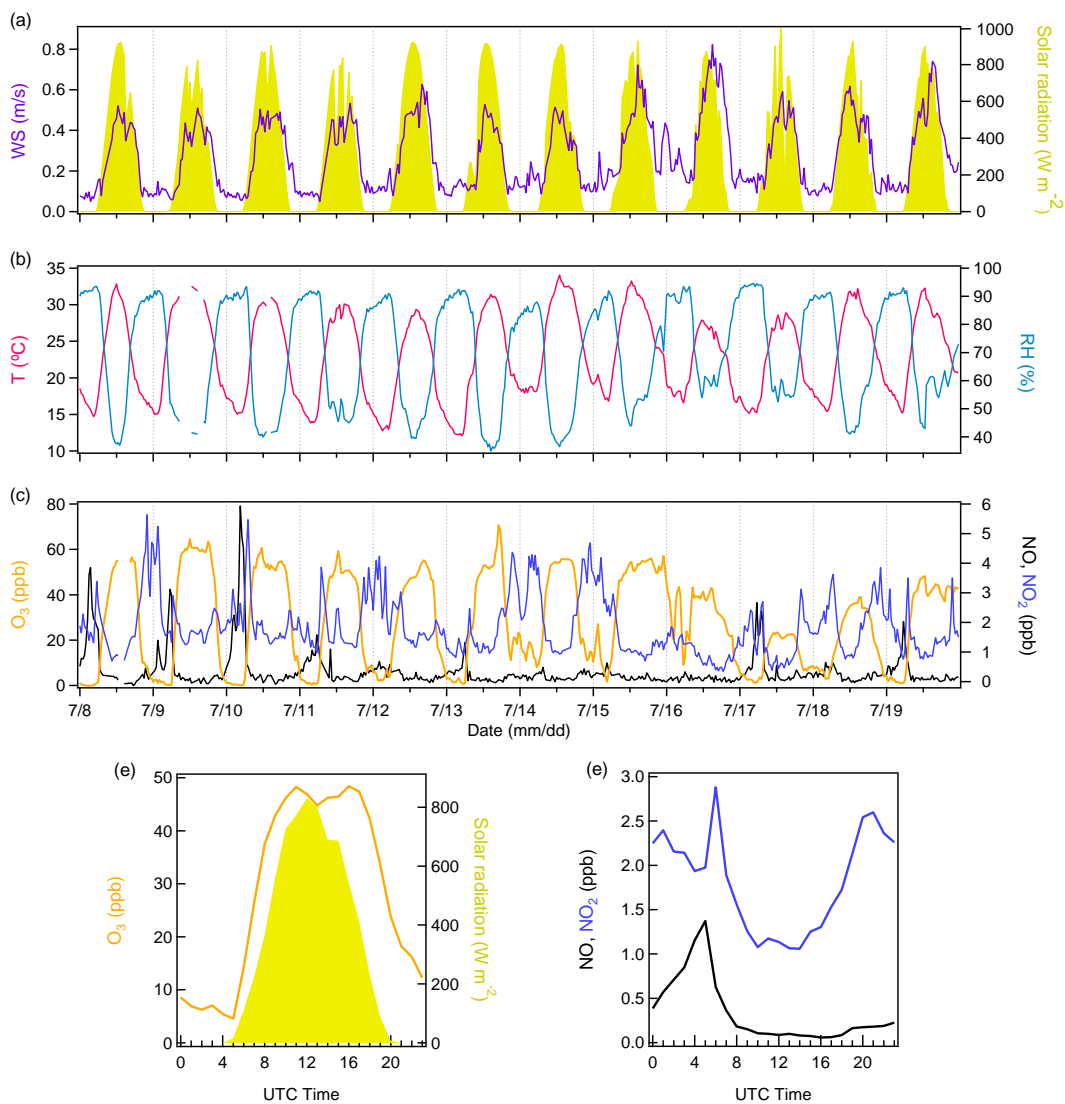
- 645 Pang, X.: Biogenic volatile organic compound analyses by PTR-TOF-MS: Calibration, humidity effect and reduced electric
646 field dependency, *Journal of Environmental Sciences*, 32, 196-206, <https://doi.org/10.1016/j.jes.2015.01.013>, 2015.
- 647 Peräkylä, O., Vogt, M., Tikkanen, O.-P., Laurila, T., Kajos, M. K., Rantala, P. A., Patokoski, J., Aalto, J., Yli-Juuti, T., Ehn,
648 M., Sipilä, M., Paasonen, P., Rissanen, M., Nieminen, T., Taipale, R., Keronen, P., Lappalainen, H. K., Ruuskanen, T. M.,
649 Rinne, J., Kerminen, V.-M., Kulmala, M., Bäck, J., and Petäjä, T.: Monoterpenes' oxidation capacity and rate over a boreal
650 forest: temporal variation and connection to growth of newly formed particles, *Boreal Environ. Res.*, 19, 293-310, 2014.
- 651 Petäjä, T., Mauldin, I. R. L., Kosciuch, E., McGrath, J., Nieminen, T., Paasonen, P., Boy, M., Adamov, A., Kotiaho, T., and
652 Kulmala, M.: Sulfuric acid and OH concentrations in a boreal forest site, *Atmos. Chem. Phys.*, 9, 7435-7448, 10.5194/acp-9-
653 7435-2009, 2009.
- 654 Pfeiffer, T., Forberich, O., and Comes, F. J.: The contribution of the ozonolysis of terpenes to tropospheric OH concentrations,
655 *Canadian Journal of Physics*, 79, 131-142, 10.1139/p01-030, 2001.
- 656 Presto, A. A., Huff Hartz, K. E., and Donahue, N. M.: Secondary Organic Aerosol Production from Terpene Ozonolysis. 2.
657 Effect of NO_x Concentration, *Environmental Science & Technology*, 39, 7046-7054, 10.1021/es050400s, 2005.
- 658 Qin, M., Hu, Y., Wang, X., Vasilakos, P., Boyd, C. M., Xu, L., Song, Y., Ng, N. L., Nenes, A., and Russell, A. G.: Modeling
659 biogenic secondary organic aerosol (BSOA) formation from monoterpene reactions with NO₃: A case study of the SOAS
660 campaign using CMAQ, *Atmos Environ*, 184, 146-155, <https://doi.org/10.1016/j.atmosenv.2018.03.042>, 2018.
- 661 Ren, X., Harder, H., Martinez, M., Leshner, R. L., Oligier, A., Shirley, T., Adams, J., Simpas, J. B., and Brune, W. H.: HO_x
662 concentrations and OH reactivity observations in New York City during PMTACS-NY2001, *Atmos Environ*, 37, 3627-3637,
663 [https://doi.org/10.1016/S1352-2310\(03\)00460-6](https://doi.org/10.1016/S1352-2310(03)00460-6), 2003.
- 664 Rickard, A. R., Johnson, D., McGill, C. D., and Marston, G.: OH yields in the gas-phase reactions of ozone with alkenes, *J*
665 *Phys Chem A*, 103, 7656-7664, 1999.
- 666 Rinne, J., Ruuskanen, T. M., Reissell, A., Taipale, R., Hakola, H., and Kulmala, M.: On-line PTR-MS measurements of
667 atmospheric concentrations of volatile organic compounds in a European boreal forest ecosystem, *Boreal Environ. Res.*, 10,
668 425-436, 2005.
- 669 Riva, M., Rantala, P., Krechmer, J. E., Peräkylä, O., Zhang, Y., Heikkinen, L., Garmash, O., Yan, C., Kulmala, M., Worsnop,
670 D., and Ehn, M.: Evaluating the performance of five different chemical ionization techniques for detecting gaseous oxygenated
671 organic species, *Atmos. Meas. Tech.*, 12, 2403-2421, <https://doi.org/10.5194/amt-12-2403-2019>, 2019a.
- 672 Riva, M., Heikkinen, L., Bell, D. M., Peräkylä, O., Zha, Q., Schallhart, S., Rissanen, M. P., Imre, D., Petäjä, T., Thornton, J.
673 A., Zelenyuk, A., and Ehn, M.: Chemical transformations in monoterpene-derived organic aerosol enhanced by inorganic
674 composition, *npj Climate and Atmospheric Science*, 2, 2, 10.1038/s41612-018-0058-0, 2019b.
- 675 Ruppert, L., and Heinz Becker, K.: A product study of the OH radical-initiated oxidation of isoprene: formation of C5-
676 unsaturated diols, *Atmos Environ*, 34, 1529-1542, [https://doi.org/10.1016/S1352-2310\(99\)00408-2](https://doi.org/10.1016/S1352-2310(99)00408-2), 2000.
- 677 Sakulyanontvittaya, T., Duhl, T., Wiedinmyer, C., Helmig, D., Matsunaga, S., Potosnak, M., Milford, J., and Guenther, A.:
678 Monoterpene and Sesquiterpene Emission Estimates for the United States, *Environmental Science & Technology*, 42, 1623-
679 1629, 10.1021/es702274e, 2008.
- 680 Schallhart, S., Rantala, P., Kajos, M. K., Aalto, J., Mammarella, I., Ruuskanen, T. M., and Kulmala, M.: Temporal variation
681 of VOC fluxes measured with PTR-TOF above a boreal forest, *Atmos. Chem. Phys.*, 18, 815-832, 10.5194/acp-18-815-2018,
682 2018.
- 683 Sekimoto, K., Li, S.-M., Yuan, B., Koss, A., Coggon, M., Warneke, C., and de Gouw, J.: Calculation of the sensitivity of
684 proton-transfer-reaction mass spectrometry (PTR-MS) for organic trace gases using molecular properties, *International Journal*
685 *of Mass Spectrometry*, 421, 71-94, <https://doi.org/10.1016/j.ijms.2017.04.006>, 2017.
- 686 Shirinzadeh, B., Wang, C. C., and Deng, D. Q.: Diurnal variation of the OH concentration in ambient air, *Geophys Res Lett*,
687 14, 123-126, 10.1029/GL014i002p00123, 1987.
- 688 Simon, V., Clement, B., Riba, M. - L., and Torres, L.: The Landes experiment: Monoterpenes emitted from the maritime pine,
689 *J. Geophys. Res.*, 99 (D8), 16501 - 16510, doi:10.1029/94JD00785, 1994.
- 690 Sindelarova, K., Granier, C., Bouarar, I., Guenther, A., Tilmes, S., Stavrou, T., Müller, J. F., Kuhn, U., Stefani, P., and
691 Knorr, W.: Global data set of biogenic VOC emissions calculated by the MEGAN model over the last 30 years, *Atmos. Chem.*
692 *Phys.*, 14, 9317-9341, 10.5194/acp-14-9317-2014, 2014.



- 693 Spanel, P., and Smith, D.: SIFT studies of the reactions of H₃O⁺, NO⁺ and O₂⁺ with a series of alcohols, *International Journal*
694 *of Mass Spectrometry and Ion Processes*, 167-168, 375-388, [https://doi.org/10.1016/S0168-1176\(97\)00085-2](https://doi.org/10.1016/S0168-1176(97)00085-2), 1997.
- 695 Stone, D., Whalley, L. K., and Heard, D. E.: Tropospheric OH and HO₂ radicals: field measurements and model comparisons,
696 *Chemical Society Reviews*, 41, 6348-6404, 10.1039/C2CS35140D, 2012.
- 697 Surratt, J. D., Chan, A. W. H., Eddingsaas, N. C., Chan, M., Loza, C. L., Kwan, A. J., Hersey, S. P., Flagan, R. C., Wennberg,
698 P. O., and Seinfeld, J. H.: Reactive intermediates revealed in secondary organic aerosol formation from isoprene, 107, 6640-
699 6645, 10.1073/pnas.0911114107 %J *Proceedings of the National Academy of Sciences*, 2010.
- 700 Tani, A., Hayward, S., and Hewitt, C. N.: Measurement of monoterpenes and related compounds by proton transfer reaction-
701 mass spectrometry (PTR-MS), *International Journal of Mass Spectrometry*, 223-224, 561-578, [https://doi.org/10.1016/S1387-3806\(02\)00880-1](https://doi.org/10.1016/S1387-3806(02)00880-1), 2003.
- 703 Tani, A., Hayward, S., Hansel, A., and Hewitt, C. N.: Effect of water vapour pressure on monoterpene measurements using
704 proton transfer reaction-mass spectrometry (PTR-MS), *International Journal of Mass Spectrometry*, 239, 161-169,
705 <https://doi.org/10.1016/j.ijms.2004.07.020>, 2004.
- 706 Tani, A.: Fragmentation and Reaction Rate Constants of Terpenoids Determined by Proton Transfer Reaction-mass
707 Spectrometry, *Environmental Control in Biology*, 51, 23-29, 10.2525/ecb.51.23, 2013.
- 708 Tsigaridis, K., and Kanakidou, M.: Global modelling of secondary organic aerosol in the troposphere: a sensitivity analysis,
709 *Atmos. Chem. Phys.*, 3, 1849-1869, 10.5194/acp-3-1849-2003, 2003.
- 710 von Schwartzberg, K., Schultze, W., and Kassner, H. J. P. C. R.: The moss *Physcomitrella patens* releases a tetracyclic
711 diterpene, 22, 780-786, 10.1007/s00299-004-0754-6, 2004.
- 712 Wei, D., Fuentes, J. D., Gerken, T., Chamecki, M., Trowbridge, A. M., Stoy, P. C., Katul, G. G., Fisch, G., Acevedo, O.,
713 Manzi, A., von Randow, C., and dos Santos, R. M. N.: Environmental and biological controls on seasonal patterns of isoprene
714 above a rain forest in central Amazonia, *Agricultural and Forest Meteorology*, 256-257, 391-406,
715 <https://doi.org/10.1016/j.agrformet.2018.03.024>, 2018.
- 716 Wennberg, P. O., Bates, K. H., Crouse, J. D., Dodson, L. G., McVay, R. C., Mertens, L. A., Nguyen, T. B., Praske, E.,
717 Schwantes, R. H., Smarte, M. D., St Clair, J. M., Teng, A. P., Zhang, X., and Seinfeld, J. H.: Gas-Phase Reactions of Isoprene
718 and Its Major Oxidation Products, *Chem Rev*, 118, 3337-3390, 2018.
- 719 Winterhalter, R., Herrmann, F., Kanawati, B., Nguyen, T. L., Peeters, J., Vereecken, L., and Moortgat, G. K.: The gas-phase
720 ozonolysis of β-caryophyllene (C₁₅H₂₄). Part I: an experimental study, *Physical Chemistry Chemical Physics*, 11, 4152-4172,
721 10.1039/B817824K, 2009.
- 722 Xiong, F., McAvey, K. M., Pratt, K. A., Groff, C. J., Hostetler, M. A., Lipton, M. A., Starn, T. K., Seeley, J. V., Bertman, S.
723 B., Teng, A. P., Crouse, J. D., Nguyen, T. B., Wennberg, P. O., Misztal, P. K., Goldstein, A. H., Guenther, A. B., Koss, A.
724 R., Olson, K. F., de Gouw, J. A., Baumann, K., Edgerton, E. S., Feiner, P. A., Zhang, L., Miller, D. O., Brune, W. H., and
725 Shepson, P. B.: Observation of isoprene hydroxynitrates in the southeastern United States and implications for the fate of NO_x,
726 *Atmos. Chem. Phys.*, 15, 11257-11272, <https://doi.org/10.5194/acp-15-11257-2015>, 2015.
- 727 Xu, L., Pye, H. O. T., He, J., Chen, Y., Murphy, B. N., and Ng, N. L.: Experimental and model estimates of the contributions
728 from biogenic monoterpenes and sesquiterpenes to secondary organic aerosol in the southeastern United States, *Atmos. Chem.*
729 *Phys.*, 18, 12613-12637, <https://doi.org/10.5194/acp-18-12613-2018>, 2018.
- 730 Yan, C., Nie, W., Äijälä, M., Rissanen, M. P., Canagaratna, M. R., Massoli, P., Junninen, H., Jokinen, T., Sarnela, N., Häme,
731 S. A. K., Schobesberger, S., Canonaco, F., Yao, L., Prévôt, A. S. H., Petäjä, T., Kulmala, M., Sipilä, M., Worsnop, D. R., and
732 Ehn, M.: Source characterization of highly oxidized multifunctional compounds in a boreal forest environment using positive
733 matrix factorization, *Atmos. Chem. Phys.*, 16, 12715-12731, 10.5194/acp-16-12715-2016, 2016.
- 734 Yáñez-Serrano, A. M., Nölscher, A. C., Bourtsoukidis, E., Gomes Alves, E., Ganzeveld, L., Bonn, B., Wolff, S., Sa, M.,
735 Yamasoe, M., Williams, J., Andreae, M. O., and Kesselmeier, J.: Monoterpene chemical speciation in a tropical
736 rainforest: variation with season, height, and time of day at the Amazon Tall Tower Observatory (ATTO), *Atmos. Chem. Phys.*,
737 18, 3403-3418, 10.5194/acp-18-3403-2018, 2018.
- 738 Yuan, B., Koss, A. R., Warneke, C., Coggon, M., Sekimoto, K., and de Gouw, J. A.: Proton-Transfer-Reaction Mass
739 Spectrometry: Applications in Atmospheric Sciences, *Chem Rev*, 117, 13187-13229, 2017.
- 740 Yucuis, R. A., Stanier, C. O., and Hornbuckle, K. C.: Cyclic siloxanes in air, including identification of high levels in Chicago
741 and distinct diurnal variation, *Chemosphere*, 92, 905-910, <https://doi.org/10.1016/j.chemosphere.2013.02.051>, 2013.

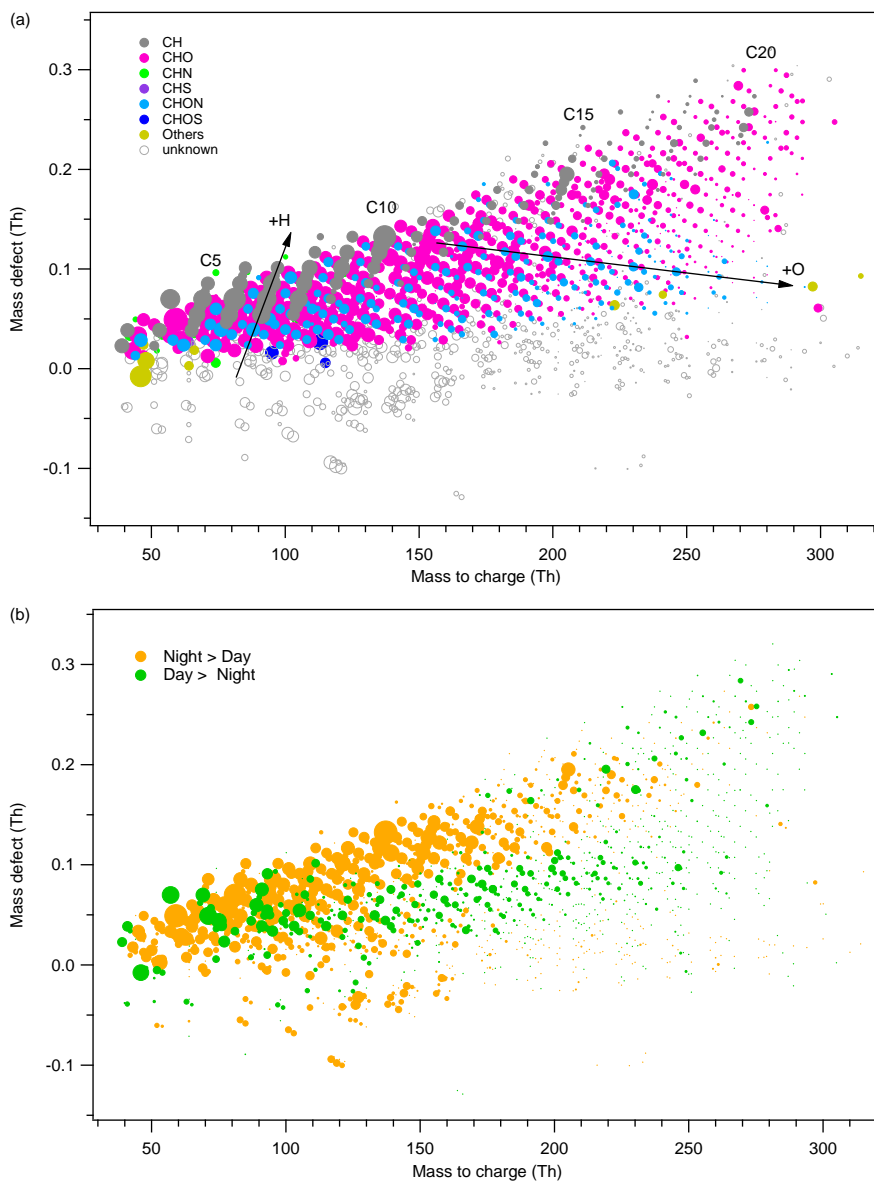


- 742 Zhang, H., Yee, L. D., Lee, B. H., Curtis, M. P., Worton, D. R., Isaacman-VanWertz, G., Offenberg, J. H., Lewandowski, M.,
743 Kleindienst, T. E., Beaver, M. R., Holder, A. L., Lonneman, W. A., Docherty, K. S., Jaoui, M., Pye, H. O. T., Hu, W., Day, D.
744 A., Campuzano-Jost, P., Jimenez, J. L., Guo, H., Weber, R. J., de Gouw, J., Koss, A. R., Edgerton, E. S., Brune, W., Mohr, C.,
745 Lopez-Hilfiker, F. D., Lutz, A., Kreisberg, N. M., Spielman, S. R., Hering, S. V., Wilson, K. R., Thornton, J. A., and Goldstein,
746 A. H.: Monoterpenes are the largest source of summertime organic aerosol in the southeastern United States, 115, 2038-2043,
747 10.1073/pnas.1717513115 %J Proceedings of the National Academy of Sciences, 2018.
- 748 Zhu, J., Penner, J. E., Yu, F., Sillman, S., Andreae, M. O., and Coe, H.: Decrease in radiative forcing by organic aerosol
749 nucleation, climate, and land use change, Nature Communications, 10, 423, 10.1038/s41467-019-08407-7, 2019.
- 750 Zhu, Y., Yang, L., Kawamura, K., Chen, J., Ono, K., Wang, X., Xue, L., and Wang, W.: Contributions and source identification
751 of biogenic and anthropogenic hydrocarbons to secondary organic aerosols at Mt. Tai in 2014, Environ Pollut, 220, 863-872,
752 <https://doi.org/10.1016/j.envpol.2016.10.070>, 2017.



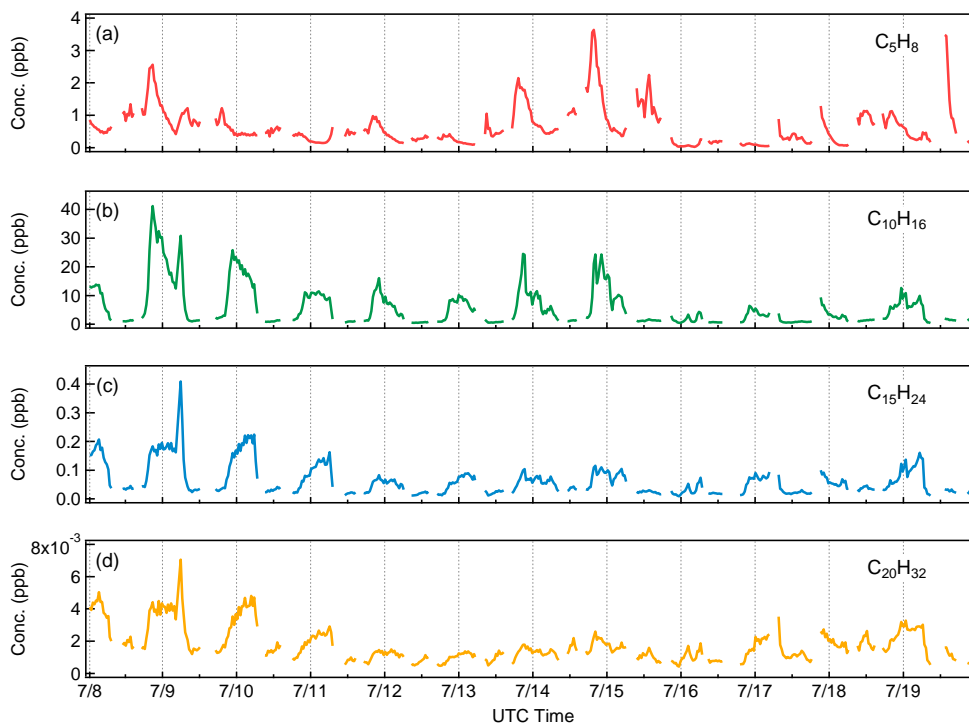
753

754 **Figure 1.** Variations of meteorological conditions and trace gases. (a) Time series of wind speed and solar radiation. (b)
755 Time series of temperature and relative humidity. (c) Time series of O_3 , NO , and NO_2 . (d) Diurnal cycles of O_3 and
756 solar radiation. (e) Diurnal cycles of NO and NO_2 .



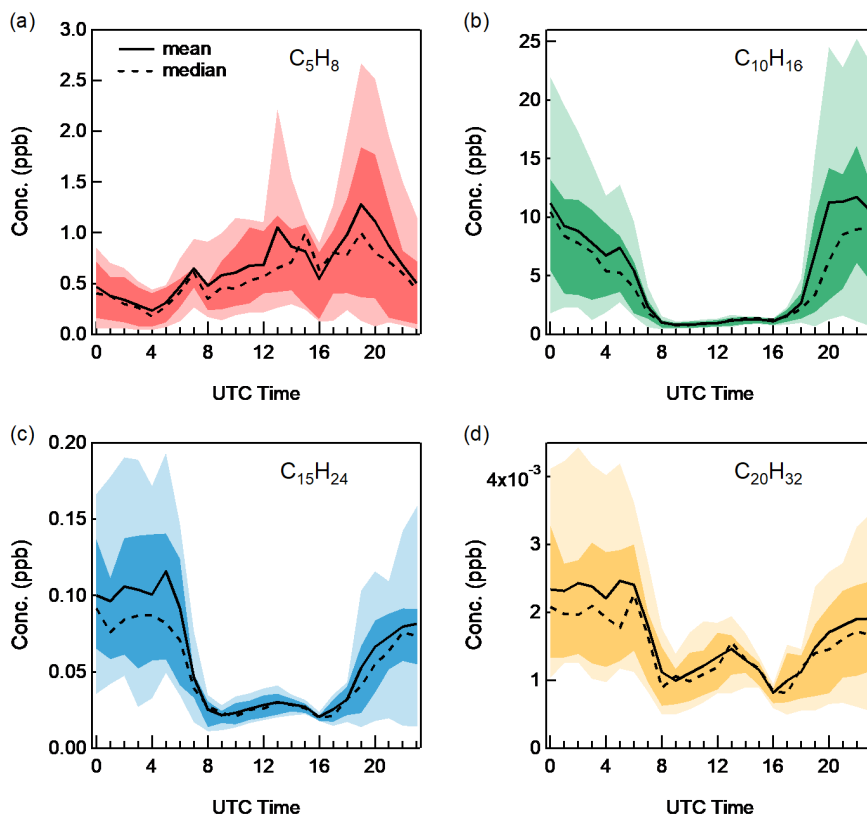
757

758 **Figure 2.** Mass defect plot of the ions identified by high-resolution analysis of Vocus PTR-TOF data set. The x-axis
759 shows the mass to charge ratio and the y-axis shows the mass defect, which is the deviation of the accurate mass from
760 the nominal mass. Data points in (a) are color-coded by ion family (CH, CHO, CHN, CHS, CHON, CHOS) and sized
761 by the logarithm of peak area. Data points in (b) are shown in orange when signals are higher during nighttime and in
762 green when daytime signal is higher. The size corresponds to the difference of daytime and nighttime signal for the
763 molecule.



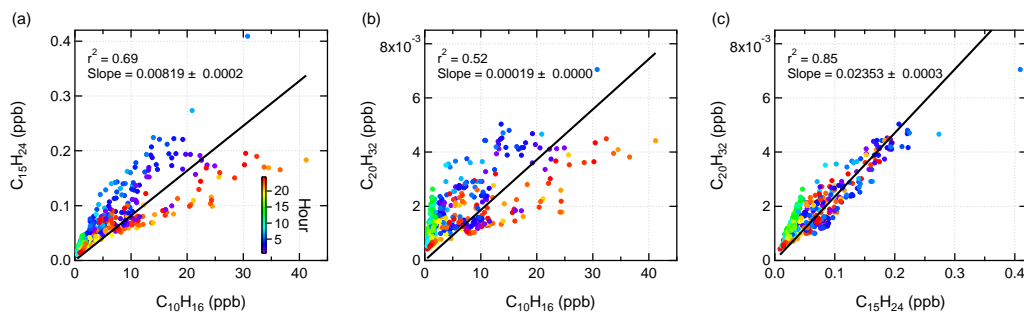
764

765 **Figure 3.** Time series of (a) C_5H_8 , (b) $C_{10}H_{16}$, (c) $C_{15}H_{24}$, and (d) $C_{20}H_{32}$.



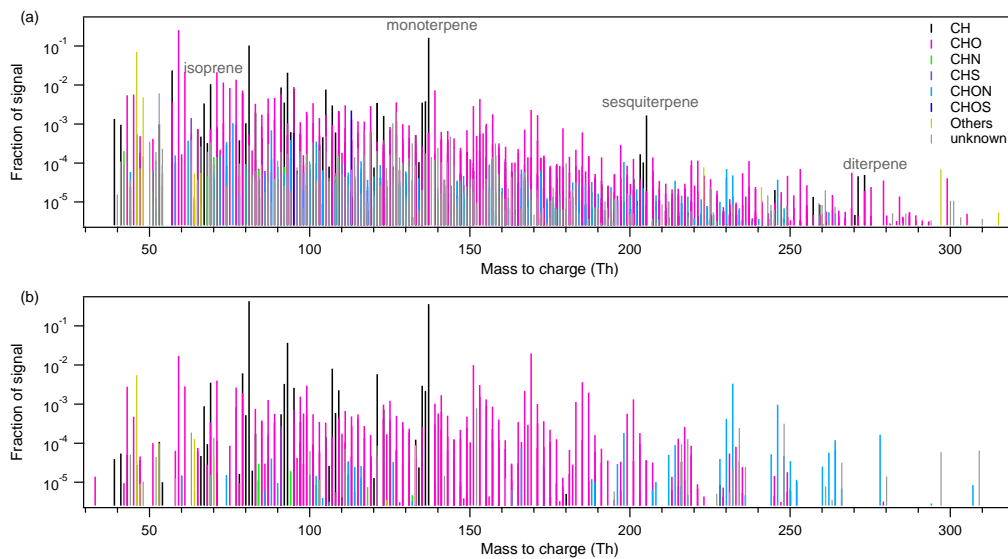
766

767 **Figure 4.** Diurnal cycles of (a) C_5H_8 , (b) $C_{10}H_{16}$, (c) $C_{15}H_{24}$, and (d) $C_{20}H_{32}$, with the 10th, 25th, 75th, and 90th percentiles
768 shown in the shaded area.



769

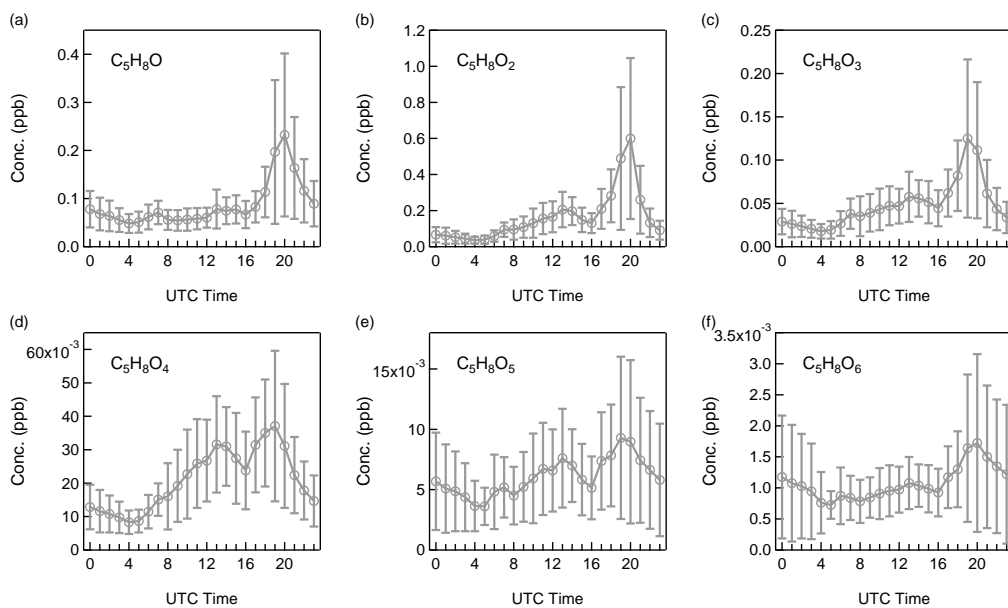
770 **Figure 5.** Scatter plots of (a) $C_{15}H_{24}$ vs. $C_{10}H_{16}$, (b) $C_{20}H_{32}$ vs. $C_{10}H_{16}$, and (c) $C_{20}H_{32}$ vs. $C_{15}H_{24}$, colored by time of the
771 day.



772

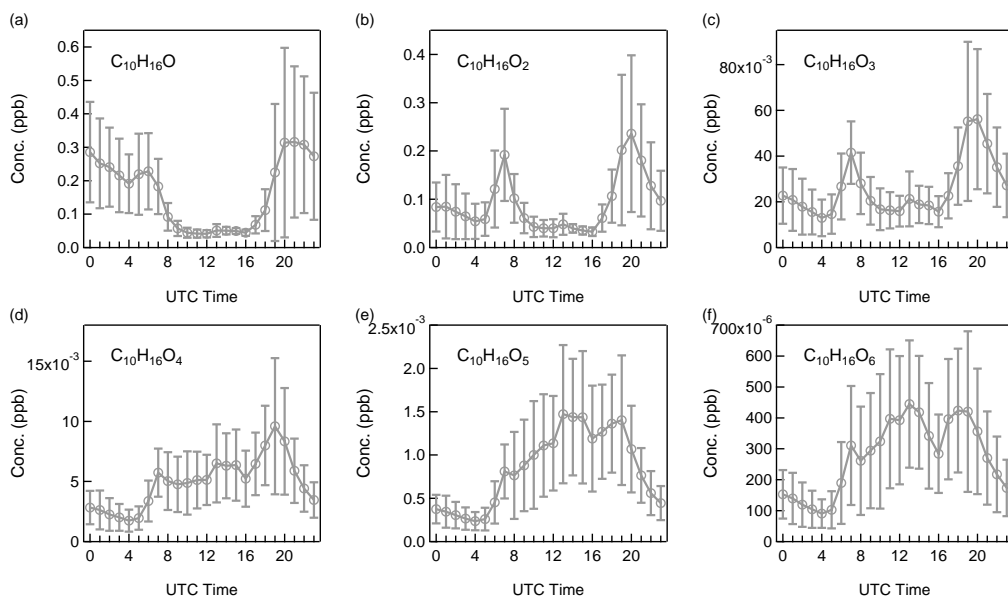
773 **Figure 6. Comparison of ambient average high-resolution mass spectra with those from α -pinene oxidation experiments**

774 **in the COALA chamber. (a) ambient observations in the Landes Forest; (b) α -pinene ozonolysis with NO_x .**



775

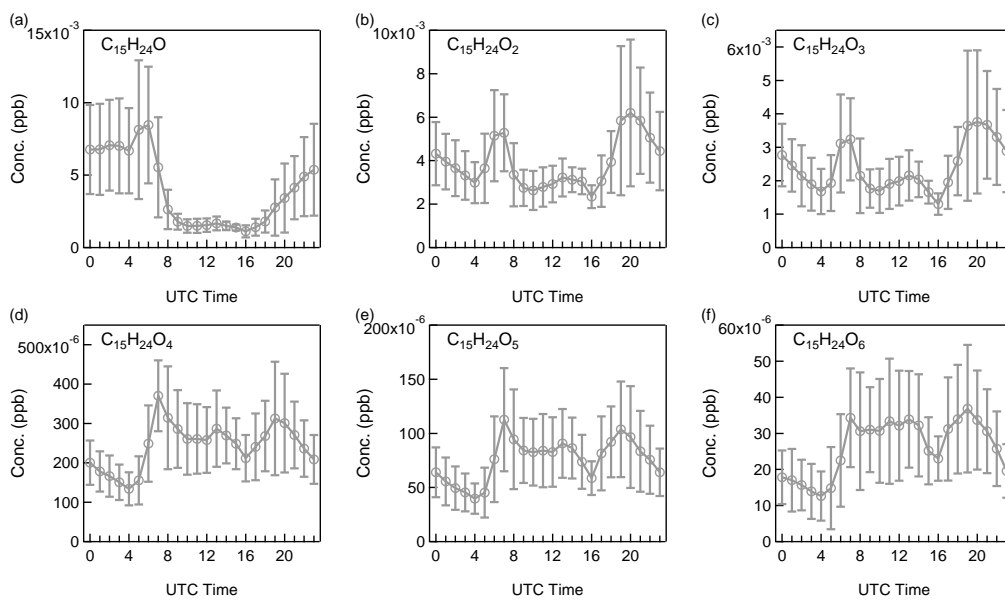
776 **Figure 7. Diurnal patterns of non-nitrate isoprene oxidation products: (a) C_5H_8O , (b) $C_5H_8O_2$, (c) $C_5H_8O_3$, (d) $C_5H_8O_4$,**
777 **(e) $C_5H_8O_5$, and (f) $C_5H_8O_6$.**



778

779 **Figure 8. Diurnal patterns of non-nitrate monoterpene oxidation products: (a) $C_{10}H_{16}O$, (b) $C_{10}H_{16}O_2$, (c) $C_{10}H_{16}O_3$, (d)**

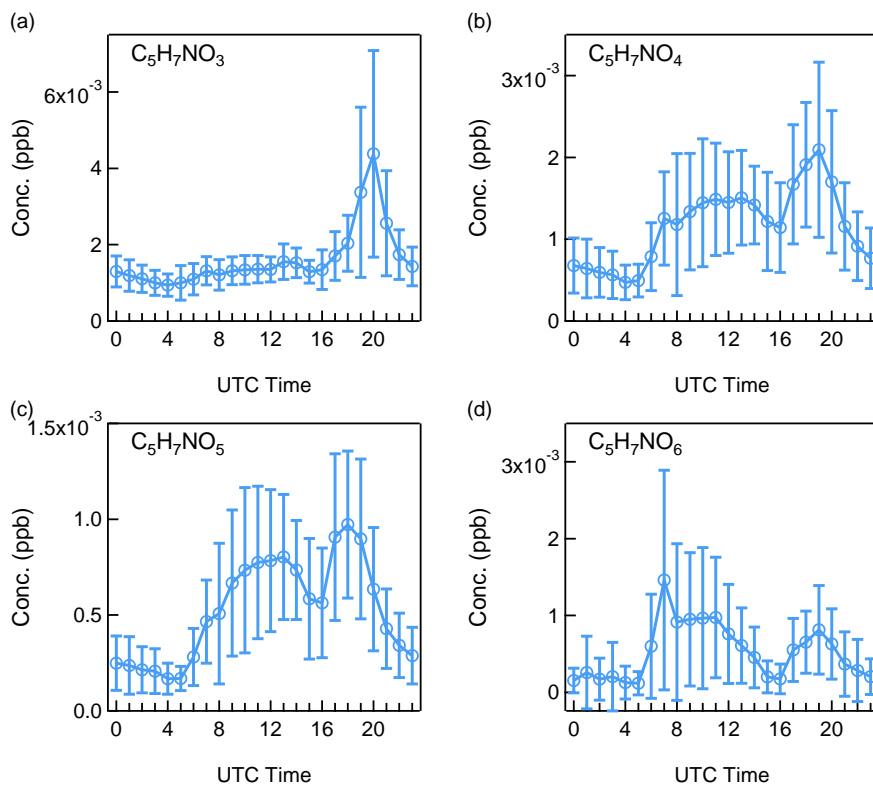
780 **$C_{10}H_{16}O_4$, (e) $C_{10}H_{16}O_5$, and (f) $C_{10}H_{16}O_6$.**



781

782 **Figure 9. Diurnal patterns of non-nitrate sesquiterpene oxidation products: (a) $C_{15}H_{24}O$, (b) $C_{15}H_{24}O_2$, (c) $C_{15}H_{24}O_3$, (d)**

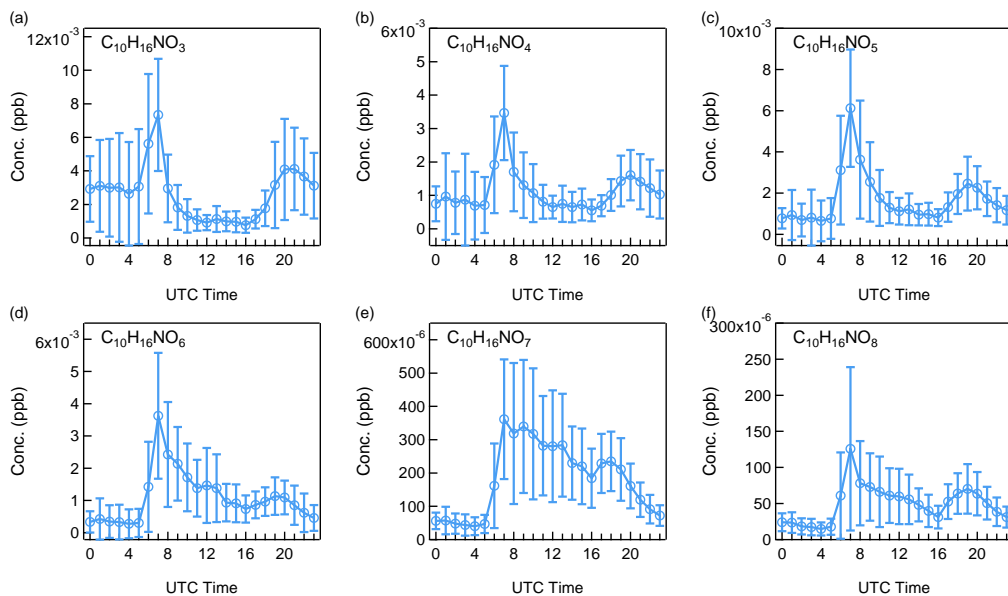
783 **$C_{15}H_{24}O_4$, (e) $C_{15}H_{24}O_5$, and (f) $C_{15}H_{24}O_6$.**



784

785 **Figure 10. Diurnal patterns of isoprene-derived organic nitrates: (a) $C_5H_7NO_3$, (b) $C_5H_7NO_4$, (c) $C_5H_7NO_5$, and (d)**

786 **$C_5H_7NO_6$.**



787

788 **Figure 11. Diurnal patterns of monoterpene-derived organic nitrates: (a) $C_{10}H_{15}NO_3$, (b) $C_{10}H_{15}NO_4$, (c) $C_{10}H_{15}NO_5$, (d)**

789 **$C_{10}H_{15}NO_6$, (e) $C_{10}H_{15}NO_7$, and (f) $C_{10}H_{15}NO_8$.**